# Online Data-Driven Optimization of Aerodynamic Performance for an Unconventional Morphing Aircraft

**MSc Thesis Aerospace Engineering**

T. Woldhuis

# Online Data-Driven Optimization of Aerodynamic Performance for an Unconventional Morphing Aircraft

MSc Thesis Aerospace Engineering

Thesis report

by

T. Woldhuis

to obtain the degree of Master of Science
at the Delft University of Technology
to be defended publicly on Thursday 7 November, 2024 at 09:00

| *Thesis committee*: | |
|---|---|
| Chair: | Dr. Ir. C. de Visser |
| Supervisors: | Dr. X. Wang |
| | Dr. S. Asaro |
| External examiner: | Dr. Ir. R. Vos |
| Place: | Faculty of Aerospace Engineering, Delft |
| Project Duration: | February, 2024 - November, 2024 |
| Student number: | 5043166 |

An electronic version of this thesis is available at
https://brightspace.tudelft.nl/d2l/le/content/560234/Home.


Faculty of Aerospace Engineering · Delft University of Technology

# Preface

This thesis is submitted in partial fulfillment of the requirements for the degree of MSc Aerospace Engineering, with a specialization in Control & Simulation. My journey into bio-inspired morphing for aerospace applications began during my Bachelor's thesis, which sparked my interest in the potential of this field. Building on that early exposure, I decided to contact Dr. Xuerui Wang again for possible MSc thesis topics, this time with a focus on Control & Simulation.

I would like to express my sincere gratitude to my thesis supervisor, Dr. Xuerui Wang, for her exceptional guidance throughout this project. Her insightful feedback and willingness to brainstorm were invaluable to the development of this work. I would also like to thank Dr. Salvatore Asaro for sharing his expertise on the Flying-V and helping me explore the practical applications of this research.

A special thanks to my family and friends, whose support has been essential throughout this journey. Lastly, I would like to acknowledge you, the reader—thank you for your interest, and I hope you find this thesis both informative and enjoyable.

- Thymen Woldhuis

# Contents

# Nomenclature

**List of Abbreviations**

BOBYQA Bound Optimization by Quadratic Approximation

CMA-ES Covariance Matrix Adaptation Evolution Strategy

DIRECT Dividing Rectangles

FTO Fault Tolerant Optimization

MTOW Maximum Takeoff Weight

RANS Reynolds-Averaged Navier–Stokes

VLM Vortex Lattice Method

**List of Symbols**

| | |
|---|---|
| $\alpha$ | Angle of attack |
| $\boldsymbol{\delta}$ | Flap deflections |
| $\rho$ | Density |
| Mach | Mach number |
| $C_D$ | Coefficient of drag |
| $C_L$ | Coefficient of lift |
| $C_M$ | Pitching moment coefficient |
| $C_{L_{\text{target}}}$ | Target Lift Coefficient |
| $F_{\text{weight}}$ | Flap Weight |
| $h$ | Altitude |
| $J$ | Cost |
| $k_1$ | Coefficient of lift deviation penalty |
| $k_2$ | Moment coefficient deviation penalty |
| $Re$ | Reynolds number |
| $U$ | Airspeed |
| $\boldsymbol{s}$ | Spline control parameters |
| $_i$ | Iteration |
| $_{opt}$ | Optimal |

# List of Figures

# Part I

## Literature Review & Research Definition

# 1

# General Introduction

In an effort to increase the efficiency of aircraft, many studies have been focusing on optimization during cruise, as it constitutes the majority of flight time. This method of working allows computationally expensive solvers to optimize the aircraft for predetermined flight conditions. However, discrepancies between simulated and actual conditions can arise when the aircraft operates outside of these optimized conditions, or when the aircraft's physical characteristics deviate from the model due to for instance manufacturing variability, icing, or structural damages. Online optimization offers a potential solution to these challenges. The primary concept behind online optimization is that the aircraft can continuously adjust its shape during flight. This is often achieved by learning and updating a surrogate model in real-time to guide the optimization process. Conventional wings with fixed flaps provide only limited optimization possibilities. In contrast, nature offers inspiration, as birds exhibit flexible wings capable of assuming a wide range of shapes. At TU Delft, Mkhoyan et al. developed a camber morphing wing [1], enabling the wing to adopt various configurations and thereby enhancing the potential for real-time shape optimization. The work done in this thesis aims to improve current optimization frameworks that are capable of optimizing the aerodynamic performance of an aircraft in real-time.

This optimization study will be done on TU Delft Flying-V. Implementation on the Flying-V poses extra challenges because besides aerodynamic optimization, the control surfaces must also keep the aircraft in longitudinal trim and allow for lateral maneuvers as there is not a separate elevator or rudder. In addition, the Flying-V present nonlinear behavior at high angles of attack which should be accounted for in the optimization strategy.

Real-time shape optimization is not a novel topic; therefore, a brief literature review is provided in Chapter 2. The research outline, including the research objective and questions, is presented in Chapter 3. The main findings of this thesis are presented in the scientific article as can be found in Part II. It is a pleasure to announce that this work has been accepted to be presented and published at the AIAA SciTech 2025 conference. Some studies have been left out of the scientific article, but still provide valuable insights into the thesis, this has been presented in Chapter 4. A conclusion of the thesis and recommendations for future work are presented in Chapter 5. Lastly, a project plan outlining the overall timeline of the thesis is shown in Appendix A.

# 2

# Literature Review

While the optimization of morphing wing shapes is a relatively new area of research, it shares many similarities with the long-standing field of trailing and leading edge control surface optimization. This topic has been extensively studied over the years. This chapter will review the literature, starting with the early work on control surface optimization in Section 2.1. Ongoing research at NASA Ames Research Center, which focuses on online shape optimization using a polynomial-based model and gradient-based optimization methods, will be discussed in Section 2.2. Additionally, recent advancements at TU Delft, where a seamless morphing wing has been developed and its shape optimization explored, will be reviewed in Section 2.3. Finally, the current knowledge gaps and the specific contributions of this thesis will be addressed in Section 2.4. Note that this literature review is a summary of the most notable studies on the topic, a more concise and relevant literature review is given in the introduction of the scientific paper.

## 2.1. Early work on real-time control surface optimization

One of the first mentions of real-time control surface optimization is that of NASA Dryden Research Center [2]. This study explored a real-time adaptive configuration optimization on an L-1011 aircraft. The aircraft used forced-response, symmetric, outboard aileron maneuvers to calculate the incremental drag. This allowed them to use a regression analysis to find the optimal settings. It achieved a drag reduction of approximately 1%. This system has only one optimizable variable, namely the outboard ailerons. The horizontal stabilizer and angle of attack were indirectly optimized to maintain trim. Due to the limited complexity of study, this optimization framework is not necessarily a topic of interest for this thesis.

In 2006, a different study demonstrated real-time drag reduction for a wing with eight leading-edge and eight trailing-edge control surfaces [3]. The key focus of the study was addressing the challenges introduced by real-time measurements, including signal noise, hysteresis, and repeatability issues in function evaluations. These problems complicated the use of conventional gradient-based optimization methods, as derivatives could not be reliably computed due to the noisy data. In response to the absence of a reliable numerical function for drag, the study implemented a generating set search (GSS) method, which is a derivative-free optimization technique. The GSS optimizer was successful in reducing drag for given angles of attack while satisfying constraints such as keeping lift constant. However, applying this system to a real aircraft presents challenges. Since all function evaluations are conducted directly on the wing, implementing this approach in flight would be impractical. As the number of control surfaces increases, the optimization runtime would not be favourable for real-time application during flight. In addition, this study was only performed on a wing model, thus challenges like keeping the aircraft in longitudinal trim were not considered.

## 2.2. Online shape optimization for Variable Camber Continuous Trailing Edge Flap (VCCTEF) systems

More recent studies on shape optimization have been performed by the NASA Ames Research Center. The first of a range of studies suggested the usage of a Variable Camber Continuous Trailing Edge Flap (VCCTEF) [4]. In 2016, a real-time least-squares drag minimization method was developed in Ref. [5]. This study proposed to use a recursive least squares algorithm to estimate the aerodynamic coefficients of the aircraft and fit it to a polynomial model. The optimal wing shape was then found using a gradient

based optimization method, namely Newton-Raphson. The advantage of this method is that the model is linear-in-the-parameters which means that optimization can be done in an iterative deterministic way. Later in 2019, this method was tested in a wind tunnel experiment and resulted in drag reduction of up to 9.4% for off-design lift coefficients [6]. Continuing from the successful tests was another study [7] that aimed to apply this method to the Boeing AR 13.5 Common Research Model which resulted in drag reduction of 1.95% to 3.37% for transsonic flight conditions. A trade-off on the ideal number of flaps has been presented in [8].

While this method is promising, there are still some limitations associated with the methodology used. Firstly, as it used a polynomial-based aircraft model, the structure of this model is fixed and can only be used near the trimming points. To have enough detail in the local regions while still being valid for global use, the degree of the polynomial would have to increase exponentially. Secondly, as the optimization problem can be nonlinear and non-convex, gradient-based optimization strategies are prone to converging to local minima and saddle points. Moreover, these methods struggle with non-smooth functions and can involve costly gradient or Hessian calculations, particularly in large-scale problems. Lastly, when an actuator failure occurred in [6], it had to be manually excluded from the control space. Ref. [9] suggested a fault tolerant system to automatically detect, adapt, and optimize the model but an implementation was never studied.

## 2.3. Global online black-box shape optimization for seamless morphing wing

A previous thesis has been conducted on online black-box shape optimization for a seamless active morphing wing [10, 11]. This study has applied optimization to the SmartX-Alpha developed by the TU Delft [1]. The algorithm was tested in a wind tunnel [11] and resulted in a drag reduction of up to 8%, and a predicted drag reduction of up to 19.8% for further studies with experimental data gathered from the wind tunnel tests. The study proposed to model the aircraft aerodynamics in real-time using radial basis function neural networks, which were optimized using covariance matrix adaptation evolution strategy (CMA-ES) [12]. However, the study was limited to only the wing. Expanding this algorithm to a full aircraft introduces extra challenges, such as keeping the aircraft in trim. Although this approach improved the transition from local to global optimization, additional improvements in computational efficiency are still needed. Genetic optimization methods typically demand a high number of function evaluations and tend to be advantageous primarily when the problem involves more than ten variables or when the search space is poorly defined. Other limitations of Ref. [10] include not having the Mach number or altitude as an input variable to the algorithm, having limited fault tolerance for when the mechanism fails, and having on-board model inaccuracies near the domain edges.

## 2.4. Proposed research direction

While great efforts have been done to realise online shape optimization for morphing wings, there are still some limitations with the current findings. So far, there has not been a global online optimization strategy made for a full free-flying aircraft. This thesis should look into an optimization framework with improved computational efficiency, enhanced performance, and better adaptability in handling time-varying, nonlinear, and non-convex problems compared to state-of-the-art methods. In addition, the morphing wing has been tested on a wing-body aircraft that faces extra challenges over normal aircraft, like pitch brake and nonlinear behaviour. Furthermore, limited research and testing has been done on actuator failure detection and optimization. Lastly, all studies tested the optimization on a single flight condition which can lead to biased results. This thesis will present the optimization study for a typical full flight.

# 3

# Research Questions

Following from the literature study, a clear research outline can be drawn. The main research objective can be stated as follows:

**Research Objective**

to improve online optimization of a trailing edge morphing wing on the TU Delft Flying-V by finding the most optimal wing shape

The research objective can be divided into three research questions, each indicating a key point of research necessary to realise the research objective.

**Research Question 1**

How to design an optimization architecture that is best suited for online shape optimization?

The optimization architecture and its subcomponents are crucial to the workings of the optimization system. Since there are several options that exist in literature the following subquestions must be answered:

1. Does the system need to be feedforward or feedback?
2. What on-board model methods are there and which is most suited for online shape optimization?
3. What optimization methods are there and which is most suited for online shape optimization?

**Research Question 2**

How can the optimizer best account for actuator failures?

With a system compromising of many actuators, one must thoroughly take into account the case of actuator failure. The system should be able to detect and adapt to any failed actuators and still be optimizable. The subquestions that are related to this are:

1. How to detect an actuator failure from the optimization loop?
2. How to spot the failed actuator and remove it from the on-board model and optimizable variables?
3. How to optimize the remaining actuators?

**Research Question 3**

Compared to non-morphing wings, what are the efficiency gains for any point in the flight profile?

Normal wings are optimized for cruise. Thus, it is expected that the optimization benefits are mostly seen in the off-target lift coefficients. This research questions aims to understand where efficiency benefits might be found and how to system actually optimizes in these conditions.

# Part II

## Scientific Article

# Online Data-Driven Optimization of Aerodynamic Performance for an Unconventional Morphing Aircraft

Thymen Woldhuis*, Salvatore Asaro†, and Xuerui Wang‡
*Delft University of Technology, Delft, 2629 HS, The Netherlands*

**In nature, birds can intelligently adapt their wing shapes to their environment. This paper aims to replicate this capability by designing an online data-driven aerodynamic performance optimization framework for an unconventional morphing aircraft. Compared to state-of-the-art methods, the proposed framework efficiently finds global optima with reduced computational load when addressing time-varying, nonlinear, and non-convex problems. It also demonstrates enhanced adaptability to unforeseen scenarios. In the event of a sudden actuator fault, the algorithm can automatically detect the fault, adapt the onboard data-driven model, and continue performing optimization and trimming tasks using the remaining healthy actuators. Additionally, the paper addresses the optimal number of actuators within a morphing surface, considering the tradeoff between optimization performance and the weight penalty. High-fidelity simulations demonstrate that through active morphing, the proposed framework achieves drag reductions of 1.9–4.9 % during cruise and up to 12.6 % at higher operational lift coefficients (due to heavier weight and lower speed), resulting in an overall drag reduction of 2.98 % over a typical flight cycle, which corresponds to fuel savings of approximately 150 kg/h. This research represents a significant advancement in sustainable aviation, contributing to reduced fuel consumption, lower emissions, and improved fault tolerance for next-generation aircraft.**

## Nomenclature

| | |
|---|---|
| BOBYQA | Bound Optimization by Quadratic Approximation |
| CMA-ES | Covariance Matrix Adaptation Evolution Strategy |
| DIRECT | Dividing Rectangles |
| FTO | Fault Tolerant Optimization |
| MTOW | Maximum Takeoff Weight |
| VLM | Vortex Lattice Method |
| RANS | Reynolds-Averaged Navier–Stokes |

| | |
|---|---|
| $\alpha$ | Angle of attack |
| $C_D$ | Coefficient of drag |
| $C_L$ | Coefficient of lift |
| $C_{L_{\text{target}}}$ | Target lift Coefficient |
| $C_M$ | Pitching moment coefficient |
| $\boldsymbol{\delta}$ | Flap deflections |
| $F_{\text{weight}}$ | Flap weight |
| $h$ | Altitude |
| $_i$ | Iteration |
| $J$ | Cost |
| $k_1$ | Coefficient of lift deviation penalty |
| $k_2$ | Moment coefficient deviation penalty |
| Mach | Mach number |
| $_{\text{opt}}$ | Optimal |
| $\boldsymbol{s}$ | Spline control parameters |
| $Re$ | Reynolds number |
| $\rho$ | Density |
| $U$ | Airspeed |

*MSc Student Aerospace Engineering, Department of Control and Operations, Faculty of Aerospace Engineering, Kluyverweg 1, 2629 HS Delft, The Netherlands, t.woldhuis@student.tudelft.nl.

†Postdoctoral Researcher, Department of Flight Performance and Propulsion, Faculty of Aerospace Engineering, Kluyverweg 1, 2629 HS Delft, The Netherlands, s.asaro@tudelft.nl.

‡Tenured Assistant Professor, Department of Aerospace Structures and Materials & Department of Control and Operations, Faculty of Aerospace Engineering, Kluyverweg 1, 2629 HS Delft, The Netherlands, X.Wang-6@tudelft.nl, Senior Member AIAA.

# I. Introduction

In modern aircraft design, offline optimization is typically performed to achieve optimal aerodynamic performance at a specific point within the flight envelope, known as the "design point". Extensive offline optimization using analytical models is then employed to determine the optimal aircraft configurations at various points in the flight envelope. These offline solutions are stored in predefined lookup tables [1]. However, when the aircraft operates under different flight conditions, the aerodynamic efficiency tends to degrade. Moreover, deviations from the nominal configuration, such as those arising from manufacturing variability, icing, and structural damage, can alter the actual aerodynamic characteristics from the ideal digital models, leading to suboptimal performance, increased fuel consumption, and emissions.

Online optimization enables real-time in-flight adjustments using actual aerodynamic data, rather than relying on static offline models. This concept is inspired by nature, where birds continuously adjust their wing shapes to optimize performance in response to changing conditions. Applying this adaptive approach to aviation allows for significant performance improvements during flight, enhancing aerodynamic efficiency across a wider range of conditions. By dynamically responding to environmental changes, online optimization offers potential benefits such as improved fuel efficiency, reduced emissions, and overall enhanced aircraft performance, providing a more effective alternative to traditional optimization methods based on idealized, pre-defined models.

With this motivation, a series of studies conducted by NASA Ames Research Center explored the online optimization of a Variable Camber Continuous Trailing Edge Flap (VCCTEF) system [2]. In 2016, a real-time least-squares drag minimization method was developed, which proposed using a recursive least-squares algorithm to estimate the aircraft's aerodynamic coefficients and fit them to a polynomial model [3]. The optimal wing shape was then determined using a gradient-based optimization method, specifically Newton-Raphson. This approach was later tested in wind tunnel experiments, resulting in drag reductions of up to 9.4 % for off-design lift coefficients [1] and was also applied to the Common Research Model (CRM) [4, 5].

While promising, these studies have several limitations. First, the use of a polynomial-based aircraft model imposes a fixed structure that is valid only near the trimming points, limiting its adaptability. Achieving detailed accuracy in local regions while preserving global validity would necessitate a substantial increase in the polynomial's degree. Second, the optimization problem for aircraft performance can be nonlinear and non-convex. Gradient-based optimization strategies may converge to local minima or saddle points, exhibit sensitivity to initialization, and progress slowly in flat regions or near ill-conditioned points. Moreover, these methods struggle with non-smooth functions and can involve costly gradient or Hessian calculations, particularly in large-scale problems.

To address these limitations, an alternative approach was proposed for the Smart-X morphing wing [6] and tested in a wind tunnel experiment [7], achieving up to 19.8 % drag reduction. This study introduced the use of radial basis function neural networks to model the aircraft's aerodynamics in real time, followed by optimization using the covariance matrix adaptation evolution strategy (CMA-ES) [8]. While this approach improved the transition from local to global optimization, further enhancements in computational efficiency are necessary. Genetic optimization methods often require a large number of function evaluations and are typically beneficial only when the number of variables exceeds ten or when the search space is poorly defined. Furthermore, although neural networks have proven effective in capturing aircraft dynamics, they operate as black-box models and impose significant computational demands.

Up to this point, we have identified several research gaps from an algorithm development perspective. It has become evident that an online, global, and computationally efficient aerodynamic performance optimization framework is required. In addition to these algorithmic challenges, challenges also arise from a practical point of view.

The first challenge pertains to the hardware configuration on which the optimization is applied. The research conducted in [6, 7] focused solely on wing optimization, neglecting challenges posed by free-flight conditions, such as maintaining trim and reserving control authority for stability and maneuverability. In contrast, the studies in [4, 5] applied optimization to free-flying aircraft, but the configurations were conventional, i.e., tube-and-wing designs. Consequently, optimizing the wing's control surface settings in these studies had limited impact on mitigating the drag penalties caused by the large fuselage.

This research aims to develop an optimization framework for the Flying-V [9], an innovative wing-body aircraft developed by TU Delft. The Flying-V has the potential to achieve a 25 % increase in efficiency compared to conventional tube-and-wing aircraft of similar size [9]. However, its implementation poses significant challenges. Due to the absence of conventional elevators and rudders, the control surfaces on the wing must perform multiple functions simultaneously, including three-axis trim, maneuverability, and performance optimization. Furthermore, Flying-V presents strong nonlinearity and non-convexity at high angles of attack, requiring an optimization strategy capable of addressing such complexity.

The second practical challenge lies in the control surfaces used to implement the optimization algorithm. Traditionally, aircraft are equipped with only one control surface per wing; however, in recent years, there has been an increase in the number of trailing-edge control surfaces. From a theoretical perspective, as the number of control surfaces increases, the degrees of freedom for precisely manipulating aerodynamic behavior also increase. This is why a distributed mini-flap configuration was proposed in [10]. However, this configuration does not ensure smooth transitions between adjacent flaps. In contrast, a seamless active morphing wing concept was introduced in [6]. Nevertheless, this research does not address the optimal number of actuators within the morphing surface area, considering the tradeoff between performance and the weight penalty of additional actuators.

Although increasing the number of actuators provides more control degrees of freedom, it also raises the likelihood of actuator faults in practice, as verified in the wind tunnel experiment in [1]. However, when an actuator fault occurred in that study, it was manually excluded from the control space. The algorithm lacked capabilities for automatic fault detection, fault tolerance, and onboard model adaptation, while still achieving optimal performance in post-fault scenarios. These aspects are particularly crucial during real-world operations and will be addressed in this paper.

In addition, the performance of the optimization algorithm is highly dependent on the operational point and the aircraft's mass. While performance improvements of up to 9.4 % and 19.8 % were achieved in [1] and [7], respectively, these numbers may be overly optimistic when considering a typical flight cycle. This is because commercial aircraft spend the majority of their time in cruise conditions, where their shape is likely to be already near optimal. A more realistic assessment of optimization performance over a typical flight cycle will be evaluated in this paper.

In light of the gaps in the literature, this paper proposes a fault-tolerant, global, online, and computationally efficient aerodynamic performance optimization framework and applies it to a nonlinear, free-flying, flying-wing morphing aircraft. The framework can automatically identify faulty actuators, adapt the onboard model, and achieve both trimming and performance optimization simultaneously using the remaining healthy actuators. It offers improved computational efficiency, enhanced performance, and better adaptability in handling time-varying, nonlinear, and non-convex problems compared to state-of-the-art methods, as demonstrated by a quantitative comparative study in this paper. Moreover, the paper addresses the optimal number of actuators for a morphing control surface, considering the tradeoff between performance and weight penalty. Finally, high-fidelity simulations demonstrate the effectiveness of the proposed framework throughout the entire flight envelope and provide a more realistic estimation of drag reduction during a typical commercial aircraft flight cycle.

The paper is structured as follows: The detailed algorithm design, on-board model, and optimizer are explained in Sec. II. The simulation results are then presented in Sec. III, followed by conclusions in Sec. IV.

## II. Methodology

This section presents the methodology used to model, simulate and optimize the system. First, subsection II.A outlines the overall optimization architecture. Subsection II.B delves into the development of the aerodynamic model, detailing how it is constructed and what flight conditions are considered. A data-driven on-board surrogate model is created in real-time which is developed in subsection II.C. The on-board model will then be used to optimize the angle of attack and actuator inputs. Subsection II.D presents the optimizer design. Finally, subsection II.E explores strategies for managing actuator faults, ensuring system robustness and continued operation under faulty conditions.

### A. Optimization architecture

The objective of the optimization is to find the best combination of the angle of attack ($\alpha$) and actuation inputs ($\boldsymbol{\delta}$) that maximize aerodynamic efficiency while satisfying the longitudinal trimming requirement. This should be achieved throughout the entire flight envelope, bridging the simulation-to-reality gap, adapting to new conditions, and tolerating unforeseen scenarios including icing, actuator faults, and structural damages. This optimization problem is nonlinear and non-convex.

The optimization problem is formulated as follows:

$$\begin{aligned} \underset{\alpha,\,\boldsymbol{\delta}}{\text{minimize}} \quad & J(\alpha,\boldsymbol{\delta}) = C_D + k_1(C_{L,\text{target}} - C_L)^2 + k_2(C_M)^2 \\ \text{subject to} \quad & \alpha \in [\alpha_{\min}, \alpha_{\max}], \\ & \boldsymbol{\delta} \in [\boldsymbol{\delta}_{\min}, \boldsymbol{\delta}_{\max}], \\ & \dot{\boldsymbol{\delta}} \in [\dot{\boldsymbol{\delta}}_{\min}, \dot{\boldsymbol{\delta}}_{\max}] \end{aligned} \tag{1}$$

where $C_L$ is the lift coefficient; $C_M$ is the pitching moment coefficient that should be zero at trim; $C_D$ is the drag coefficient to be minimized for reducing fuel consumption and emissions. $k_1$ and $k_2$ are user-defined weights.

The morphing surface is subject to position and velocity constraints of ± 20 deg and 45 deg/s, respectively [11]. The position constraint is further tightened to ± 16 deg in optimization to reserve margins for maneuvers. The number of actuators in $\boldsymbol{\delta}$ is treated as a variable to be optimised, intending to answer the research question of what is best number of actuators within the morphing surface. The angle of attack $\alpha$ is constrained to $\alpha \in [0, 10]$ deg for stall and pitch break protection.

Figure 1 presents the optimization architecture in a schematic view. This paper considers the mass (Mass), Mach number (Ma), and altitude ($h$) as flight condition definition variables. From this, the corresponding $C_{L_{\text{target}}}$ is calculated using Eq. (2), where the aircraft weight $W$ is balanced by lift. The computed $C_{L_{\text{target}}}$ acts as an input of the optimization loop, in which an optimizer minimizes the cost function based on a surrogate onboard model. The choice of the optimizer will be detailed in subsection II.D. To reduce computational loads of the optimizer and to ensure spanwise smoothness of the morphing surface, a spline function is created to map the real actuator motions to a virtual spline-curve. Once an optimal combination of $\alpha_i$ and spline coefficient vector $\boldsymbol{s}_i$ are found, they are then converted back to the physical actuation angles $\boldsymbol{\delta}_i$ to be used by the on-board surrogate model. In this paper, the on-board surrogate model is trained by datasets generated by real-world wind tunnel experiments and simulations based on Reynolds-Averaged Naiver–Stokes (RANS) equations and Vortex Lattice Method (VLM). The aerodynamic coefficient estimated by the on-board model are then used by the cost function.

The optimization loop is run until the optimizer converges to an optimal $\alpha_{\text{opt}}$ and $\boldsymbol{\delta}_{\text{opt}}$, then the suggested morphing configuration is tested on the real aircraft and the on-board model is updated online.

$$C_{L_{\text{target}}} = \frac{2W}{\rho U^2 S} \tag{2}$$

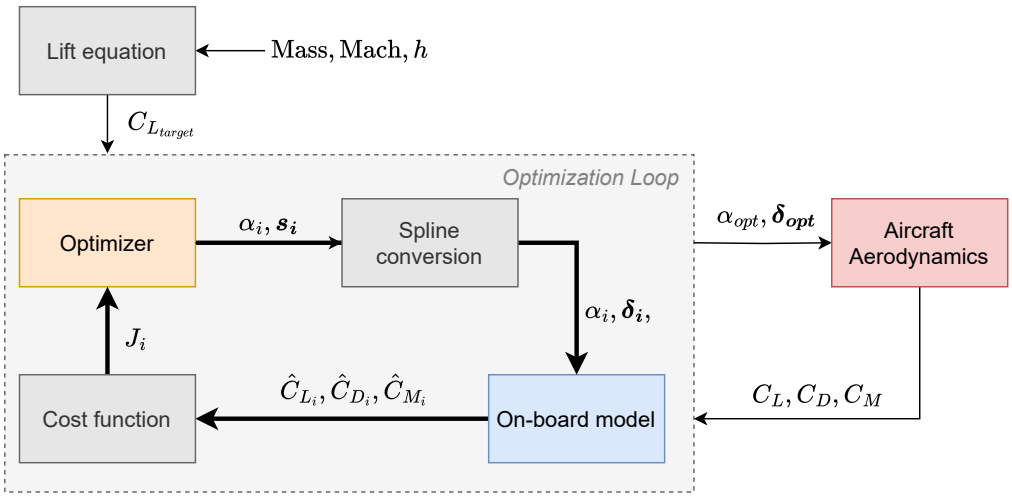


**Fig. 1 Online shape optimization architecture.**

### B. Aerodynamic model of the Flying-V

The Flying-V aircraft has an unconventional configuration as presented in Fig. 2 with the morphing surface area highlighted in yellow. Because of its tailless configuration, the morphing surfaces are responsible for multiple objectives including trimming, maneuver control, and online aerodynamic shape optimization. The morphing concept adopts the seamless Translation Induced Camber (TRIC) Smart-X Alpha in [6].

The Flying-V presents nonlinear behavior at high angles of attack and has transonic cruise speeds, leading to nonlinear, non-convex, and viscous behaviours. Therefore, high-fidelity simulations based on Reynolds-Averaged Navier–Stokes equations (RANS) are performed in the range of Ma = 0.2 to Ma = 0.7 [13]. This data is used as a

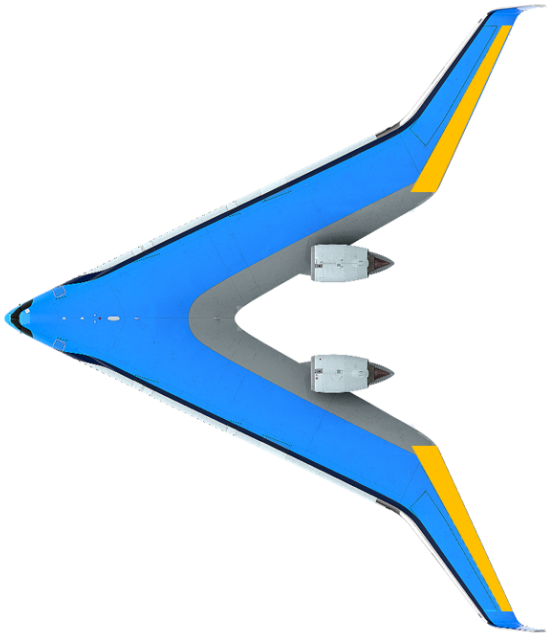

**Fig. 2 The Flying-V aircraft with morphing surface area indicated in yellow (modified from [12]).**

basis for the zero-degree angle of attack coefficients and the coefficients with respect to $\alpha$. To capture the aerodynamic mapping from actuation inputs to the coefficients, RANS simulations can also be performed. However, this would be computational inefficient because we treat the number of actuators as a variable in this paper, leading to a large number of possible compositions. To enhance computational efficiency, the contribution of the morphing surface is captured by VLM simulations. The limitations of VLM is rather minimized in this case because of the relative small area and rear location of the morphing surfaces. Finally, the simulation is calibrated with experimental data by multiplying the $C_{L_\delta}$, $C_{D_\delta}$, and $C_{M_\delta}$ coefficients by the corrections factors $a$, $b$, and $c$, as shown in the Appendix. The construction of the aerodynamic model is summarized in Fig. 3.

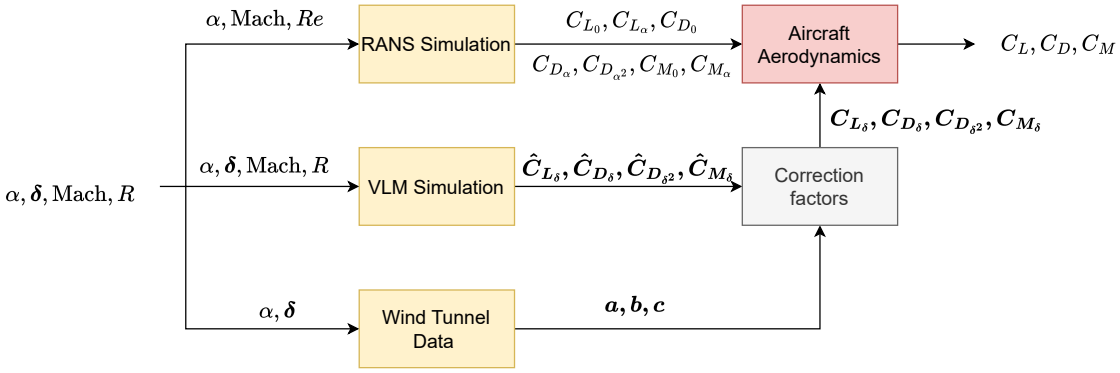


**Fig. 3 The construction of the aerodynamic model of the Flying-V aircraft.**

As mentioned before, the ideal number of actuators on the wing is set as a variable to be optimized and will be explored in subsection III.A. To ensure that morphing along the span is smooth and to reduce the number of input variables for the optimizer, the virtual shape function can be used to map the real actuator deflections to the coefficients of virtual shape functions. The state-of-the-art practice is to adopt Chebyshev polynomials [14] as virtual shape functions [3, 15]. However, the parameters used to tune the Chebyshev polynomial are coupled and changing one

parameter has a global influence on the shape of the polynomial. This hinders the state-of-the-art approach from precisely manipulating the aerodynamic properties at specific local locations. In view of this gap, this research adopts the univariate spline function as the base of virtual shape functions, which allows precise local manipulation and also ensures smooth transient in between adjacent actuators. Figure 4 shows an example of actuator deflections governed by the univariate spline curve. A tradeoff was made regarding the number of spline control coordinates by increasing the number of control points and calculating the mean squared error (MSE) between 1000 random functions and their spline approximations. It was observed that after five control points, the improvement in approximation accuracy became negligible. Therefore, the number of spline parameters was set to five.

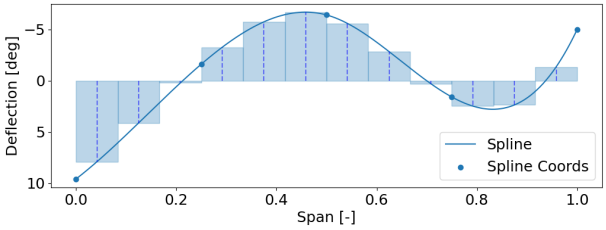


**Fig. 4 Example of an univariate spline curve smoothly connects 12 morphing actuators.**

The flight conditions considered are given in Table 2 and are based on the available data from Ref. [13]. The min ($C_{L_{\text{target}}}$) and max ($C_{L_{\text{target}}}$) are calculated using Eq. (2) and the Flying-V parameters in Table 1. The min ($C_{L_{\text{target}}}$) indicates the condition where the mass is minimal, thus MTOW minus the fuel weight and the max ($C_{L_{\text{target}}}$) uses maximum weight, thus the MTOW.

**Table 1 Aircraft modelling parameters of the Flying-V.**

| Variable | Value | Unit |
|---|---|---|
| Wing surface | 898 | $m^2$ |
| Mean aerodynamic chord | 18 | m |
| Center of gravity | 28.1 | m |
| Maximum Takeoff Weight (MTOW) | 278000 | kg |
| Fuel weight | 109000 | kg |

**Table 2 Flight conditions considered for a typical Flying-V flight profile.**

| | $h$ (m) | $\rho$ (kg/m) | $U$ (m/s) | Mach | $Re$ (10e6) | min ($C_{L_{\text{target}}}$) | max ($C_{L_{\text{target}}}$) |
|---|---|---|---|---|---|---|---|
| *Take-off/Landing* | 0 | 1.225 | 68.06 | 0.2 | 83.9 | **0.651** | **1.071** |
| | 0 | 1.225 | 85.07 | 0.25 | 105 | **0.417** | **0.685** |
| | 0 | 1.225 | 102.09 | 0.3 | 126 | **0.289** | **0.476** |
| *Climb/Descend* | 3250 | 0.886 | 131.03 | 0.4 | 124 | **0.243** | **0.399** |
| | 5450 | 0.701 | 159.34 | 0.5 | 125 | **0.207** | **0.341** |
| | 7650 | 0.547 | 185.73 | 0.6 | 119 | **0.196** | **0.322** |
| *Cruise* * | 9750 | 0.426 | 210.39 | 0.7 | 110 | **0.196** | **0.322** |

### C. On-board data-driven model

To accelerate online computation, a data-driven global on-board surrogate model is learned from the aerodynamic datasets. Various approaches are available, including polynomial-based, spline-based, and neural network models

*This condition does not represent the real cruise condition of the Flying-V. Rather, the highest Mach number for which accurate data is present.

[16], each offering distinct advantages. To determine the most suitable system identification model for this study, a thorough analysis of the requirements is essential. First, the model must be global in scope, capable of capturing nonlinear behavior. Second, it must be adaptive, allowing for updates as new data becomes available. Finally, it must be computationally efficient, with minimal evaluation costs.

Polynomial models are frequently employed for system identification due to their simplicity. However, their accuracy declines when applied to nonlinear systems [17]. Additionally, polynomial models require data collected across a wide range of global variations to accurately represent the system. In contrast, neural networks are capable of modeling both global and complex behavior. Several studies have utilized neural networks to develop on-board models [18, 19]. Despite this, neural networks are computationally demanding and often rely on global basis functions [20]. Moreover, they lack transparency [21] and are prone to numerical instabilities [22].

Multivariate splines, by contrast, have been shown to effectively generate a global aircraft model [16, 23–25], and in the case of the Flying-V, under specific test conditions, they have even outperformed other identification methods [26]. Spline-based models are composed of piecewise functions, allowing different sections of the model to be fitted independently without interference. This characteristic is particularly advantageous for global models that require high accuracy in local regions, especially around trimming points.

The independent input parameters for the on-board model are angle of attack ($\alpha$), control surface deflections ($\boldsymbol{\delta}$), and Mach number (Ma). Altitude is coupled with the Mach number, such that the appropriate altitude is selected based on Table 2 for a given Mach number. If all $\boldsymbol{\delta}$ values were used as variables in the multivariate spline, the model's complexity would increase rapidly. Therefore, the on-board model employs two separate methods. First, for each Mach number (Mach = 0.2, 0.3, 0.4, 0.5, 0.6, 0.7), a cubic univariate spline is fitted for $C_L - \alpha$, $C_D - \alpha$, and $C_M - \alpha$. Linear interpolation is then used to estimate the splines for intermediate Mach numbers. To account for the influence of the actuators, estimates for $C_{L_\delta}$, $C_{D_\delta}$, $C_{D_{\delta^2}}$, and $C_{M_\delta}$ are generated based on the aerodynamic data. This strategy mirrors the approach used to generate the aerodynamic data of the onboard model; nevertheless, in a real-world scenario, the aerodynamic data can be directly obtained during flight.

A cubic spline is defined by a cubic polynomial on each interval $[x_i, x_{i+1}]$, such that:

$$S(x) = a_i(x - x_i)^3 + b_i(x - x_i)^2 + c_i(x - x_i) + d_i, \quad \text{for} \quad x_i \leq x < x_{i+1} \tag{3}$$

where $a_i, b_i, c_i, d_i$ are the coefficients of the cubic polynomial on the $i$-th interval. For the spline to be smooth, it must be continuous on three conditions. Firstly, the spline function must be continuous at each knot to ensure the function remains gap-free.

$$S(x_i^-) = S(x_i^+) \quad \forall i \tag{4}$$

Secondly, the first derivative of the spline must be continuous at each knot to ensure no abrupt changes of the slope.

$$S'(x_i^-) = S'(x_i^+) \quad \forall i \tag{5}$$

Lastly, the second derivative must be continuous at each knot to ensure smooth curve transitions.

$$S''(x_i^-) = S''(x_i^+) \quad \forall i \tag{6}$$

To fit the on-board model, the system must be excited, for which several methods are discussed in the literature. Ref. [3] proposed applying bounded randomized deflection inputs to the aircraft model, after which the on-board model is trained. Ref. [1] introduced the sweep excitation method, which deflects all control surfaces in an ordered sweeping motion, offering greater computational efficiency and time savings compared to the random excitation method. Additionally, Ref. [15] proposed a wandering phase method, which employs pseudo-random sample points using a Sobol sequence [27]. The principle behind all excitation methods is that they are performed once during a test flight, after which the model is fine-tuned and adapted during real flights. If the model remains accurate following the previous flight, further excitations may not be necessary. This study adopts the sweep method due to its computational efficiency, while acknowledging that any of the aforementioned methods could be suitable for the proposed optimization framework. Assuming a maximum actuator velocity of 45 deg/s [11], with the actuators starting and ending at the zero position, it would take 1.42 seconds per actuator to perform the sweep excitation method. This assumes that the sampling rate of the aerodynamic coefficients is significantly higher than the excitation frequency of the actuators.

Using the sweep method, a dataset was generated from the aerodynamic model, to which the on-board model was fitted. Figure 5 illustrates the influence of Mach number on the aircraft. Markers in the figure indicate points from the

dataset to which a spline is fitted. The moment coefficient has been calculated using the center of gravity from Table 1. The nonlinear behavior is clearly visible in the $C_M$-$\alpha$ graph, where the unstable pitch break phenomenon appears at high angle of attack. In addition, the pitch break margin also decreases as Mach number increases. Figure 6 depicts the influence of actuator deflections on the aircraft when Mach number is 0.7. Upward deflection of the actuators decreases the lift coefficient but increases the moment coefficient, while downward deflection has the opposite effect. The drag coefficient increases symmetrically with both upward and downward deflection, as $C_{D_\delta} \approx 0$.

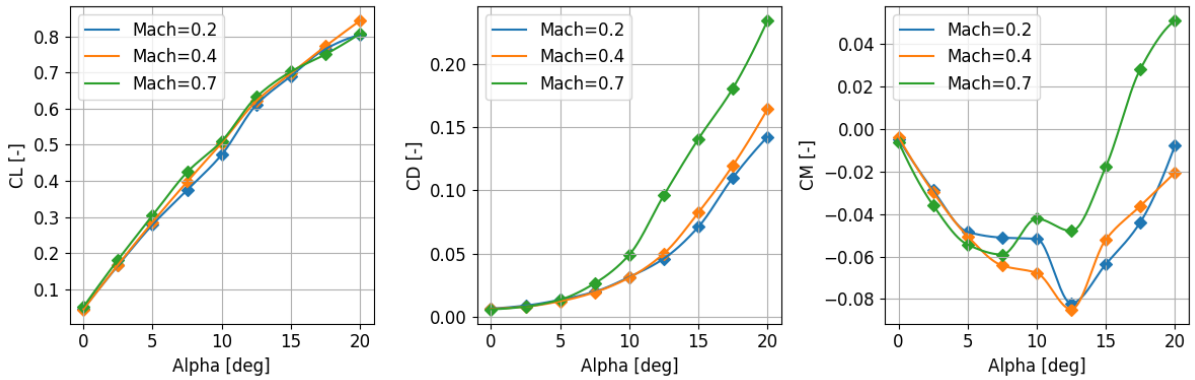


**Fig. 5 Impacts of Mach number on lift, drag, and pitching moment coefficients.**

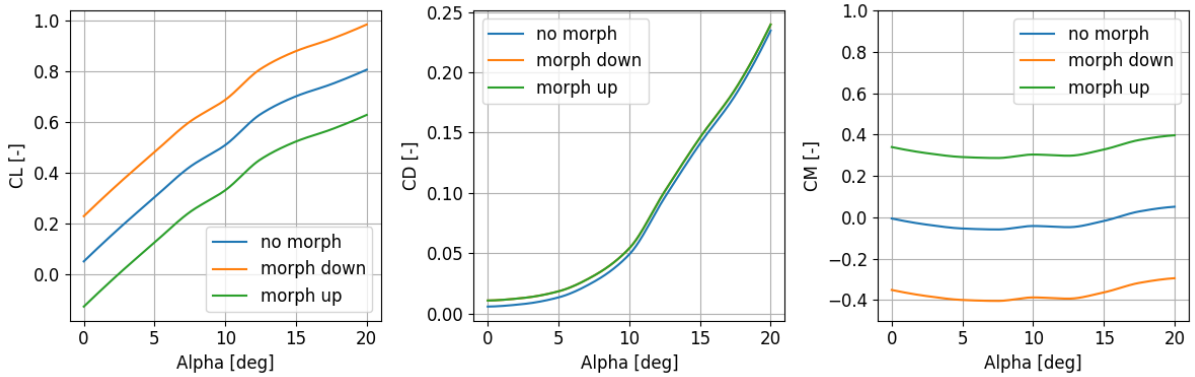


**Fig. 6 Influence of actuator deflections on aerodynamic coefficients at $\delta = -16$ deg, $\delta = 0$ deg, and $\delta = 16$ deg.**

A crucial requirement for an online optimizer is that the on-board model must be capable of adapting during flight. This implies that trustworthy fresh data points should update the model, even if they sometimes contradict the existing model. To facilitate this, a forgetting mechanism is incorporated into the on-board model. If a new data point is within a small distance of an existing one, the older point is discarded, and the spline is refitted. Fig. 7 illustrates the process of updating the model from an initial configuration. The aerodynamic coefficients, $C_L$, $C_D$, and $C_M$, are plotted against the angle of attack. The model is then updated using new, randomly generated data points, which consist of vectors of actuator deflections and angle of attack. These figures demonstrate that the model can effectively adjust its structure based on the incorporation of new data.

### D. Optimizer

To solve the problem formulated in subsection II.A, an optimizer is designed. Optimizers can generally be classified as either local or global. From a theoretical point of view, the Flying-V aerodynamic model is nonlinear and non-convex. To confirm this, we first applied a local gradient-based optimization algorithm with random initial conditions, which indeed reveals various local optima. As a result, local optimization is not suitable, and a global optimizer is required.

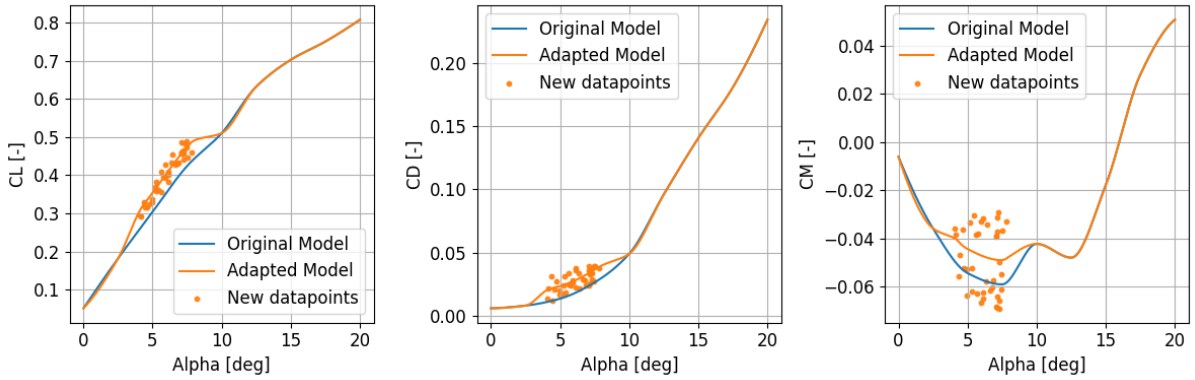


**Fig. 7 On-board model adaptation to 40 new datapoints at Mach = 0.7.**

Numerous global optimization strategies exist [28], each with distinct strengths and weaknesses. Selecting the most appropriate depends on the specific characteristics and behavior of the cost function. As previously mentioned, the on-board model is non-convex and, being spline-based, is a smooth function. Reference [29] studied various optimization algorithms for non-convex and smooth cost functions [29]. Based on this study, the tradeoff will consider on Covariance Matrix Adaptation Evolution Strategy (CMA-ES) [8], Bound Optimization by Quadratic Approximation (BOBYQA) [30], Dividing RECTangles (DIRECT) [31], and the particle swarm pattern search method (PYSWARM) [32] as viable optimization methods.

The optimizers are compared based on performance, the number of required evaluations, and sensitivity. The results of this comparison are shown in Fig. 8a. CMA-ES and BOBYQA converge to the same optimum; however, BOBYQA achieves this with fewer required function evaluations. In contrast, DIRECT and PYSWARM, which also show highly variable results, both converge to a lower optimal value.

When updating the on-board model, more complex behavior emerges due to the potential for nonlinear and non-convex behavior in local regions. To prevent significant deviations from the optimum, the optimizers must return results with low variability. By using an initial coarse on-board model and introducing random data points, the variability of the solutions can be analyzed. As illustrated in Fig. 8b, CMA-ES and BOBYQA performed similarly. Despite that, BOBYQA converges with much fewer function evaluations. Therefore, this study considers BOBYQA the most suitable optimizer for this application.

BOBYQA is a derivative-free optimization algorithm designed for solving smooth, bound-constrained, nonlinear optimization problems. It belongs to the class of trust-region algorithms, meaning it iteratively constructs local quadratic approximations of the objective function within a defined "trust region" around the current solution. The BOBYQA algorithm initializes using samples of the cost function, usually $n + 2$ (where $n$ is the number of function variables) and then approximates the objective function ($f(x)$) using a quadratic model ($Q(x)$), which can be written as:

$$Q(x) = c + g^\top (x - x_0) + \frac{1}{2}(x - x_0)^\top H (x - x_0) \tag{7}$$

where: $x_0$ is the current point (the center of the trust region); $g$ is the gradient approximation; $H$ is the Hessian approximation; $c$ is a constant term. The algorithm minimizes the quadratic model within a trust region defined by the radius $\Delta_k$. The sub-problem to solve is:

$$\min Q(x) \quad \text{subject to} \quad \|x - x_k\| \leq \Delta_k \tag{8}$$

where $\Delta_k$ is the radius of the trust region, and $x_k$ is the current best estimate. If the solution to the sub-problem improves the objective function sufficiently, the trust region is expanded; otherwise, it is shrunk. After each iteration, the algorithm uses new function evaluations to update the quadratic model $Q(x)$ around the new current best estimate.

BOBYQA is particularly well-suited for problems involving noisy data, nonlinear smooth functions, bound constraints, and low to medium dimensionality. While heuristic methods perform well in cases with a large number of optimization variables and a broad search space, this specific use case involves only six optimization variables and a well-defined search space. Moreover, because BOBYQA employs a systematic optimization approach, it typically achieves faster convergence compared to heuristic methods.

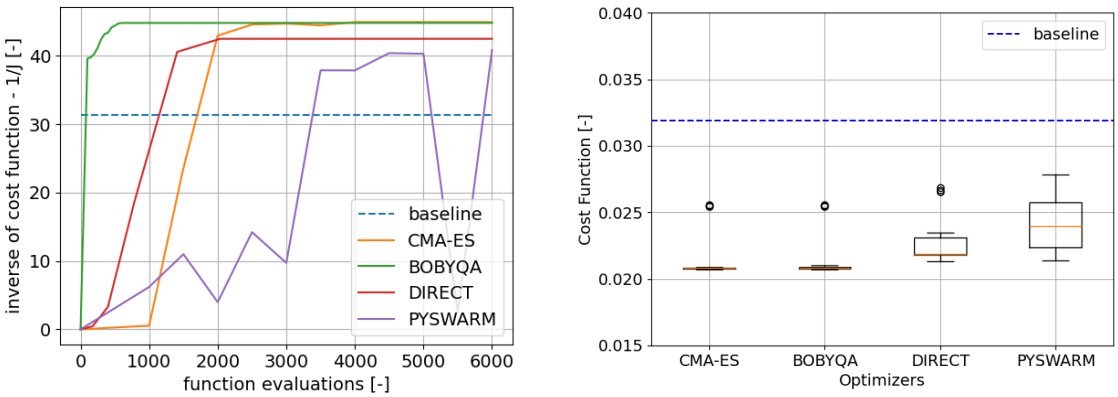


**(a) Optimizer performance against the number of function evaluations.** **(b) Variability in optimal cost for different optimizers when adapting the on-board model with new datapoints.**

**Fig. 8 Comparison of various global optimizers in terms of performance, efficiency and sensitivity.**

### E. Fault tolerance of actuator faults

The aim of fault tolerance is to detect any possible actuator failure based on fresh data and adjust the remaining actuators so that the system remains trimmed and optimized for minimal drag.

Figure 9 shows how the system identifies and optimizes in presence of an actuator failure. A checking function is designed to judge if the aircraft is actually trimmed. If an unforeseen actuator failure presence, a mismatch between the onboard model and reality would appear, leading to a derivation from the real optimum.

If the aircraft is not trimmed correctly, despite the optimizer still thinking the aircraft is in an optimum based on existing knowledge, the proposed algorithm would first identify the faulty actuator through a new model excitation sequence. If the actuator is stuck, then the identified $C_{L_\delta}$ would be approximately zero. Once the system has identified the faulty actuator, the splines will be adjusted to incorporate this fixed point, ensuring that the faulty actuator remains in the same position in the model while ensuring spanwise smoothness. The algorithm will then determine the optimal positions for the remaining actuators, taking into account the position of the faulty actuator. Figure 10 illustrates how the splines are modified to accommodate the faulty actuator. The dashed line represents the faulty actuator location, and it is evident how the splines consistently pass through this fixed point while allowing the other actuators to remain variable.

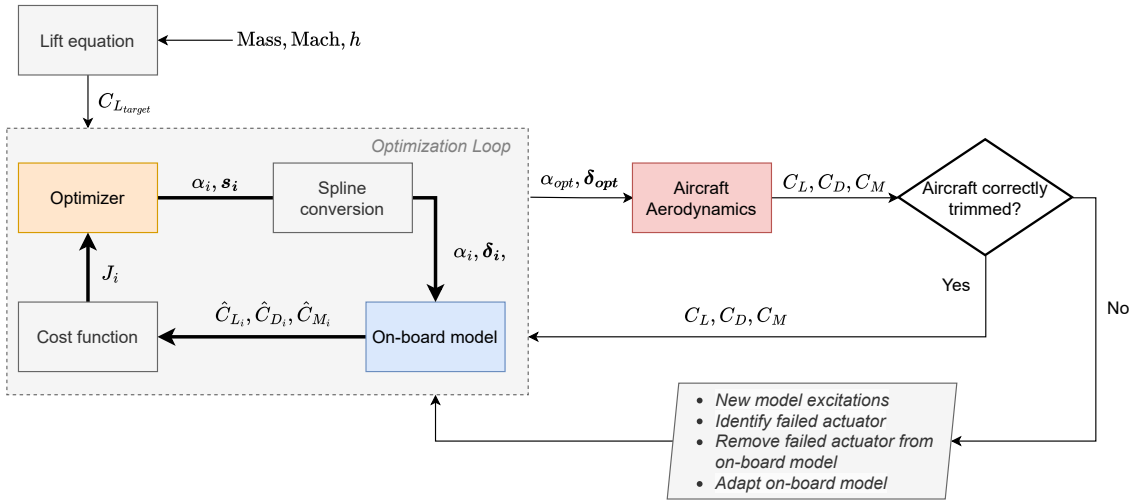


**Fig. 9 The optimization architecture that can identify and tolerate actuator faults.**

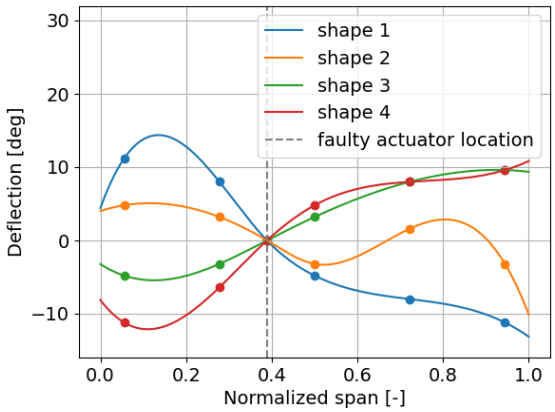


**Fig. 10 Illustration of actuator deflections based on the spline curve accounting for a faulty actuator.**

## III. Results

In this section, the effectiveness of the proposed optimization architecture is presented. Subsection III.A determines the optimal number of actuators considering the tradeoff between performance and weight penalty. Subsection III.B presents the optimization effectiveness on various flight conditions. Subsection III.C presents the fault tolerance results. Subsection III.D evaluates the overall performance improvement in one typical flight profile.

### A. Ideal number of morphing actuators

In conventional aircraft design, each wing typically has only one control surface, namely the aileron, responsible for roll control. However, as aircraft design evolves, we are seeing an increasing number of control surfaces on aircraft wings. The more control surfaces available, the greater the degrees of freedom for control, which allows for more precise manipulation of local aerodynamic properties and potential improvements in aerodynamic performance. Recently, Boeing has expressed interest in distributed trailing-edge control surfaces [10]. However, adding more control surfaces also results in a weight penalty. This subsection aims to quantify this tradeoff.

A previous study on continuous trailing-edge actuators estimated the actuator weight to be approximately 20 kg, based on calculations for both the structural weight and the servo-actuator weight [33]. However, since the tradeoff is highly dependent on the actuator weight, the efficiency benefits provided by the actuators relative to the added weight are shown in Fig. 11 for three different actuator weight scenarios.

It can be seen from Fig. 11 that as the number of actuators increases, the drag coefficient initially decreases significantly, before exhibiting a moderate upward trend. The optimal number of actuators is 9 when the single actuator weight is $F_{\text{weight}} = 10$ kg and changed to 6 for $F_{\text{weight}} = 20$ kg and $F_{\text{weight}} = 40$ kg. Considering the slopes in Fig. 11, the optimal number of actuators can be relaxed to 8 when $F_{\text{weight}} = 10$ kg and to 5 when $F_{\text{weight}} = 40$ kg without experiencing significant performance loss. In general, as the weight of each individual actuator increases, the optimal number of actuators decreases, while the drag coefficient increases. This is explained by the dependency of $C_{L_{\text{target}}}$ on aircraft weight (Eq. (2)). Namely, when the aircraft becomes heavier, higher angle of attack is required to trim the aircraft, which results in increased lift-induced drag.

### B. Optimization performance

This subsection presents the performance of the proposed optimization architecture. First, at one specific cruise condition, three approaches are compared: 1) the baseline, which is the practical state-of-the-art that only uses one single flap/actuator on each wing for trim; 2) the gradient-based optimizer based on the Nelder-Mead method; 3) the proposed global optimization method BOBYQA. The latter two approaches both use a wing with 9 actuators, and a actuator weight of 10 kg. For a fair comparison, the flight condition and control surface area for the three methods are identical.

The on-board model is initially configured with a sweeping model excitation to get the aerodynamic coefficients at

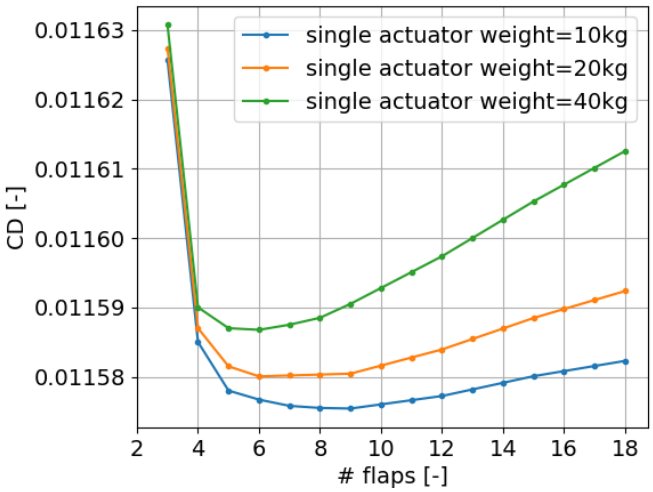


**Fig. 11 Drag reduction effectiveness against the number of actuators.**

Mach = 0.7 and $h$ = 9750 m. Then, the optimization is run on the on-board surrogate model. The number of iterations is limited to 1300 or until the minimal tolerance is met. Since the minimum tolerance is met in both cases, running the same experiment for more iterations will not change the final values. As seen from Fig. 12, both Nelder-Mead and BOBYQA present an improvement as compared to the baseline. However, the gradient-based Nelder-Mead optimization method is not capable of converging to the global optimal solution and is prone to be trapped in local optima. The spikes in the BOBYQA method are the exploration phases of the approximation regions.

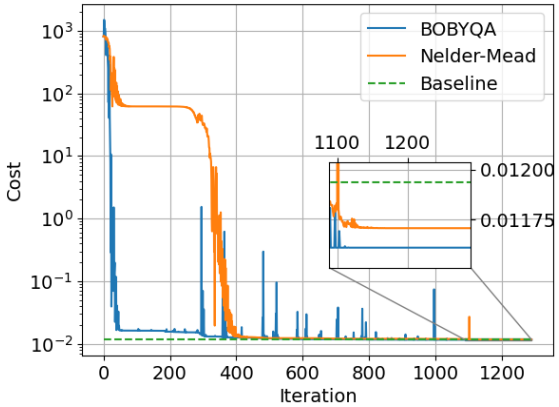


**Fig. 12 Optimization performance comparisons at a cruise condition.**

The comparison with the baseline is further detailed in Fig. 13. Since this baseline approach only has two inputs ($\alpha$, and one single actuators) to satisfy both lift and moment trim, there is only one feasible solution. It can be seen that the optimized solution has a higher $L/D$ than the simple trim solution, while keeping both the moment and lift coefficient at the intended value. At the flight condition of $C_{L_{\text{target}}}$ = 0.26 and Mach = 0.7, the proposed approach is able to increase the aerodynamic efficiency ($L/D$) by 3.08 %. This is by virtue of the distributed actuators configuration that can modify the aerodynamic profile regionally. Specifically, the outboard actuators have a larger moment arm to the center of gravity, while having a smaller influence on lift and drag. The optimizer can therefore use more of the outboard actuators to trim without over-deflecting the inner actuators, which minimizes the drag. In addition, having the inner actuators be able to deflect downwards increases the lift and therefore lowers the angle of attack, which is also

beneficial for reducing lift-induced drag.

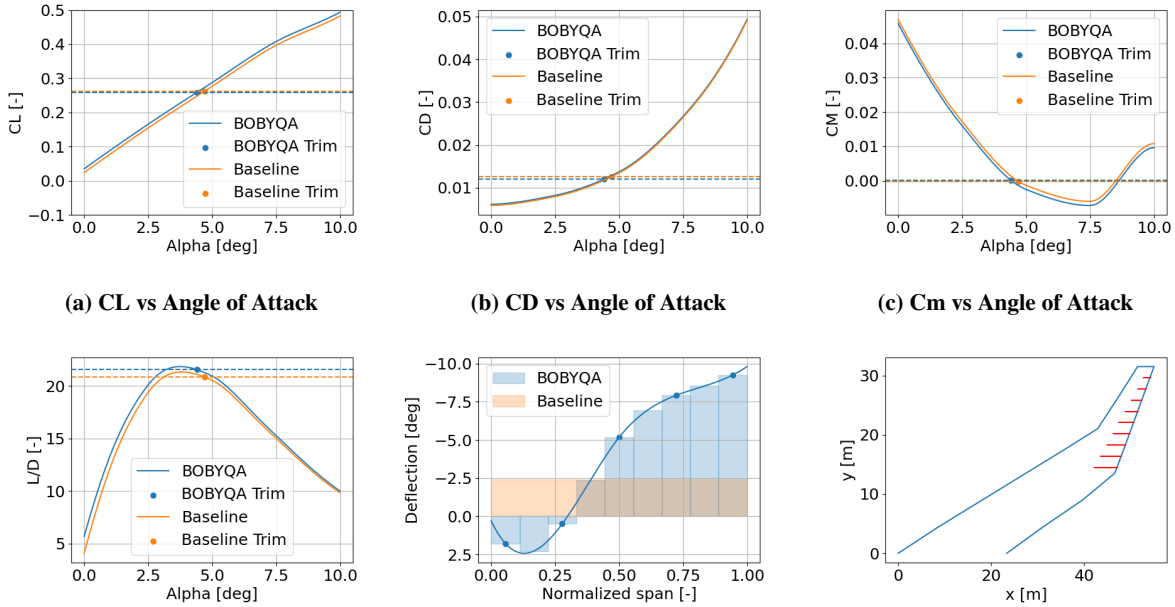


**(a) CL vs Angle of Attack** **(b) CD vs Angle of Attack** **(c) Cm vs Angle of Attack**

**(d) L/D vs Angle of Attack** **(e) Deflections** **(f) Morphing actuator locations**

**Fig. 13 Optimization results compared to the baseline for $C_{L_{\text{target}}} = 0.26$, Mach = 0.7**

After achieving a 3.08 % of aerodynamic efficiency enhancement at $C_{L_{\text{target}}} = 0.26$ and Mach = 0.7, the effectiveness of the proposed approach on various flight conditions is then evaluated in Fig. 14. The target lift coefficient is an indication of flight conditions and is related to aircraft weight, fuel burn, and flight phases. It can be seen from Fig. 14a that the optimized solution outperforms the baseline at all the tested conditions. Moreover, the optimizer gains more as the target lift coefficient increases, reaching an increase 8.19% at $C_{L_{\text{target}}} = 0.4$. When going to even higher target lift coefficients, the L/D ratio increase even reaches 12.6%. The main reason for this is that at lower target lift coefficients the system is easier to be trim with just one actuator because the ideal shape, as can be seen in Fig. 14b, is more similar to a horizontal straight line. Conversely, at higher target lift coefficients, a single-flap system loses excessive lift in its attempt to maintain a zero $C_M$, necessitating a higher angle of attack, which in turn increases drag.

Figure 15 illustrates the increase in $L/D$ ratio and the corresponding actuator configurations for different Mach numbers. The $L/D$ ratio increases at higher Mach numbers, even in the baseline case. The optimization benefits remain relatively consistent across the range of Mach numbers. It is important to note that under identical flight conditions, the $C_{L_{\text{target}}}$ increases at lower Mach numbers due to the reduction in speed. As shown in Fig. 14, a higher $C_{L_{\text{target}}}$ would lead to greater increases in the L/D ratio. However, to ensure a meaningful comparison across different Mach numbers, the $C_{L_{\text{target}}}$ is maintained at a constant value. Figure 15b indicates that the actuators require less upward morphing at higher Mach numbers because of the increase in control effectiveness.

### C. Fault tolerant optimization

In the presence of an unforeseen actuator fault, the system should still be able to optimize and trim the aircraft. This subsection presents the results of a case study where the system is optimized on the original on-board model while there is actually an unforeseen actuator fault present. The faulty actuator is simulated by setting the $C_{L_\delta}$, $C_{M_\delta}$, and $C_{D_{\delta^2}}$ in the original dataset to zero.

Figure 16 compares the results with and without fault-tolerant optimization. It shows that because of the lack of knowledge of the fault, the spline curve for the system without fault tolerance does not go through the failed actuator's actual position, leading to an untrimmed and non-optimal solution as highlighted in Fig. 16c. By contrast, the algorithm proposed in subsection III.C is able to automatically identify which actuator is stuck as well as the jammed position, thus still fulfills the optimization and trim requirements effectively.

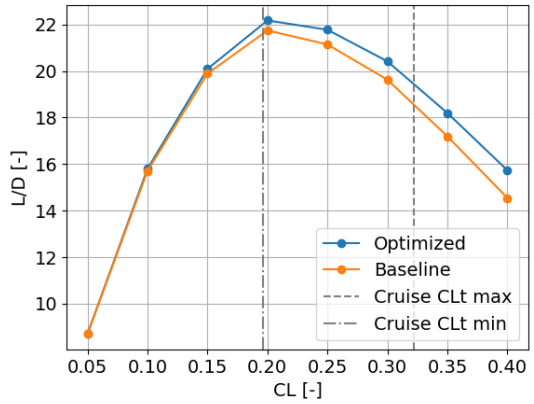


(a) Optimization for various $C_{L_{\text{target}}}$ during cruise.

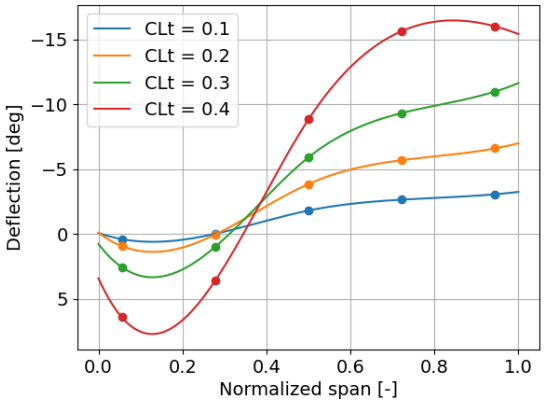


(b) Optimal shape for different $C_{L_{\text{target}}}$ during cruise.

**Fig. 14 Optimization performed for various target lift coefficients.**

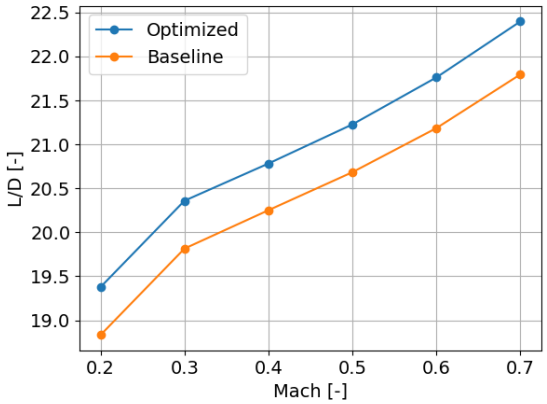


(a) Optimization for different Mach numbers.

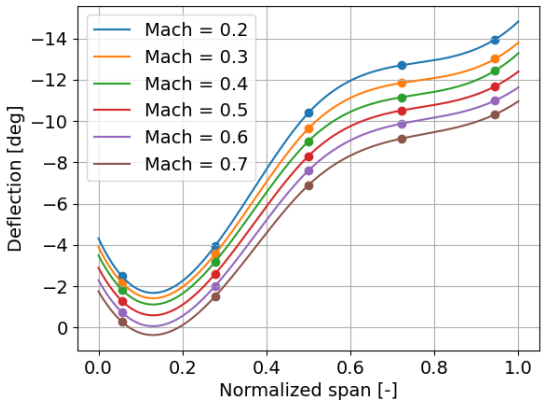


(b) Optimal shape for different Mach numbers.

**Fig. 15 Optimization performed for various Mach numbers when $C_{L_{\text{target}}} = 0.26$.**

### D. Full-flight study

In subsection III.B, the effectiveness of the proposed method on various flight conditions has been demonstrated. Depending on the flight condition, the algorithm can achieve 0% to 12.6% of increase in aerodynamic efficiency ($L/D$) and 0% to 12.6% of drag reduction ($C_D$). Nevertheless, during one typical flight cycle, an aircraft experiences different durations in different flight conditions. For example, for most of the time, the aircraft is cruising. This subsection aims to evaluate the effectiveness of the proposed method during one typical flight cycle.

A typical flight profile is considered based on data provided in Ref. [34] for the Airbus A350-9000. The results are presented in Table 3. The time per flight phase has been calculated using rate of climb/descent data from Ref. [34]. Without loss of generality, this research considers a ten-hour flight. The drag reductions is calculated for every flight phase, and a time-weighted average is calculated, resulting in a drag reduction of 2.98% in one typical flight cycle.

For jet aircraft, fuel consumption is proportional to the thrust required, so if drag decreases, thrust and fuel consumption decrease proportionally. An estimation on the fuel savings can be made using the data from Table 3. Assuming the Airbus A350-9000 consumes around 5000 kg/h of fuel, this would result in 150 kg/h of fuel saving in one typical flight cycle. For the typical flight mentioned in Table 3, this leads to a total of 1500 kg fuel savings during cruise, and 80.5 kg in other flight phases.

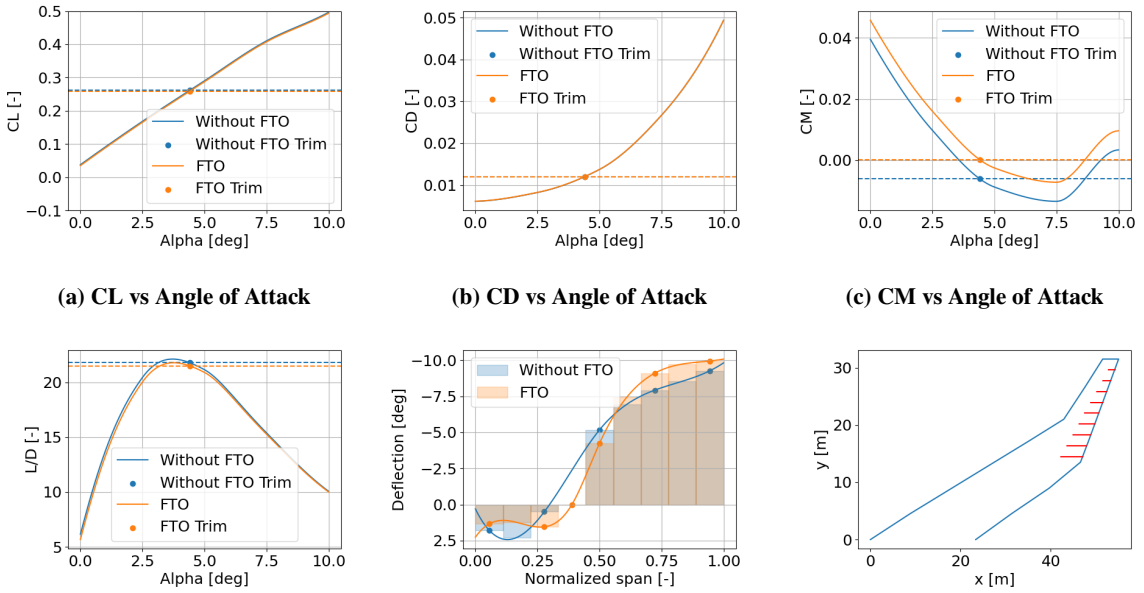


**(a) CL vs Angle of Attack** **(b) CD vs Angle of Attack** **(c) CM vs Angle of Attack**

**(d) L/D vs Angle of Attack** **(e) Deflections** **(f) Morphing actuator locations**

**Fig. 16 Optimized results for fault tolerant optimization (FTO) when$C_{L_{\text{target}}}$ = 0.26, Mach = 0.7**

**Table 3 Full flight savings for a typical flight profile with 10 hour cruise. Flight profile is based on [34].**

| | Time [min] | Mach | $C_{L_{\text{target}}}$ estimate | $C_D$ baseline | $C_D$ optimized | $\Delta C_D$ % |
|---|---|---|---|---|---|---|
| Take-off | 1.00 | 0.2 | 1.07 | 0.1758 | 0.1754 | 0.23 |
| Initial Climb | 1.67 | 0.4 | 0.40 | 0.02311 | 0.02229 | 3.59 |
| Climb to cruise | 9.97 | 0.55 | 0.33 | 0.01747 | 0.01680 | 3.84 |
| Cruise | 600.00 | 0.7 | 0.26 | 0.01266 | 0.01228 | 2.98 |
| Descent | 10.57 | 0.55 | 0.26 | 0.01320 | 0.01281 | 2.98 |
| Approach | 6.67 | 0.4 | 0.24 | 0.01202 | 0.01172 | 2.52 |
| Landing | 1.00 | 0.2 | 0.65 | 0.07227 | 0.06762 | 6.44 |
| **Total** | 630.88 | **-** | **-** | - | - | **2.98** |

## IV. Conclusions

This paper proposes a global online data-driven aerodynamic performance optimization framework, which can efficiently and smoothly model nonlinearities, adapt to changes on-board in real-time, and automatically detect and adapt to actuator faults.

Quantitive comparison results based on a free-flying Flying-V aircraft model confirm that the adopted data-driven Bound Optimization by Quadratic Approximation algorithm outperforms gradient-based local as well as other considered global optimization methods. Moreover, a multivariable spline-based on-board model effectively captures the nonlinearities of the Flying-V model and adapts to new data. Furthermore, the framework shows effectiveness in determining the optimal number of flaps considering the tradeoff between aerodynamic performance and weight penalty.

By optimizing the angle of attack and actuator positions, the proposed online optimization framework can achieve a drag reduction of 1.9 % to 4.9 % during cruise. At higher target lift coefficients (caused by heavier weight and lower speed), the drag reduction can reach up to 12.6 %. This framework has shown effectiveness throughout the entire flight envelope. For a typical flight cycle of ten hours, it can achieve a 2.98 % of drag reduction and which is approximately 150 kg/h of fuel. Last but not least, in the presence of unforeseen actuator faults, the proposed algorithm is able to automatically identify, adapt, trim, and optimize.

In conclusion, the proposed online aerodynamic performance optimization framework demonstrates significant drag reduction and fault-tolerance capabilities. This advancement represents a crucial step towards more sustainable aviation, contributing to reduced fuel consumption and lower emissions in future aircraft designs.

## Appendix

Table 4 presents the coefficients in relation to the actuator deflection from the wind tunnel data and VLM data and presents the correction factors for each section. Wind tunnel data was gathered for a three-actuator layout [13], where the controllable surface is divided into three individual sections. Any actuator of the VLM simulations that fall within the geometric bounds of a wind tunnel actuator configuration will be corrected in the same manner.

**Table 4 Correction factors for control effectiveness.**

| Coefficient | Wind tunnel | VLM | Correction Factors |
|---|---|---|---|
| $C_{L_{\delta_1}}$ | 2.59e-3 | 5.02e-3 | 0.52 |
| $C_{L_{\delta_2}}$ | 1.88e-3 | 2.13e-3 | 0.88 |
| $C_{L_{\delta_3}}$ | 1.18e-3 | 1.22e-3 | 0.97 |
| $C_{D_{\delta_1^2}}$ | 1.32e-5 | 1.05e-5 | 1.25 |
| $C_{D_{\delta_2^2}}$ | 6.75e-6 | 3.99e-6 | 1.69 |
| $C_{D_{\delta_3^2}}$ | 4.89e-6 | 2.70e-6 | 1.81 |
| $C_{M_{\delta_1}}$ | -2.80e-3 | -6.21e-3 | 0.45 |
| $C_{M_{\delta_2}}$ | -2.41e-3 | -3.73e-3 | 0.65 |
| $C_{M_{\delta_3}}$ | -1.63e-3 | -2.65e-3 | 0.62 |

## Acknowledgments

The authors would like to acknowledge Professor Roelof Vos for sharing the Flying-V aerodynamic model. In addition, the authors would like to thank the TU Delft ASM department and FAST Delft University Fund for providing funding to present at the AIAA SciTech 2025 Forum.

## References

[1] Nguyen, N., Cramer, N., Hashemi, K., Ting, E., Drew, M., Wise, R., Boskovic, J., Precup, N., Mundt, T., and Livne, E., "Real-time adaptive drag minimization wind tunnel investigation of a flexible wing with variable camber continuous trailing edge flap system," *AIAA Aviation 2019 Forum*, , No. June, 2019, pp. 1–47. https://doi.org/10.2514/6.2019-3156.

[2] Nguyen, N., "NASA Innovation Fund 2010 Project Elastically Shaped Future Air Vehicle Concept," *NASA Technical report*, 2010. https://ntrs.nasa.gov/citations/20110023698.

[3] Ferrier, Y., Nguyen, N., and Ting, E., "Real-time adaptive least-squares drag minimization for performance adaptive aeroelastic wing," *34th AIAA Applied Aerodynamics Conference*, 2016, pp. 1–33. https://doi.org/10.2514/6.2016-3567.

[4] Vassberg, J. C., DeHaan, M. A., Rivers, S. M., and Wahls, R. A., "Development of a common research model for applied CFD validation studies," *Collection of Technical Papers - AIAA Applied Aerodynamics Conference*, , No. August, 2008. https://doi.org/10.2514/6.2008-6919.

[5] Nguyen, N., and Xiong, J., "Real-time drag optimization of aspect ratio 13.5 common research model with distributed flap system," *AIAA Scitech 2021 Forum*, , No. January, 2021, pp. 1–17. https://doi.org/10.2514/6.2021-0069.

[6] Mkhoyan, T., Thakrar, N. R., Breuker, R. D., and Sodja, J., "Design and development of a seamless smart morphing wing using distributed trailing edge camber morphing for active control," *AIAA Scitech 2021 Forum*, 2021, pp. 1–16. https://doi.org/10.2514/6.2021-0477.

[7] Mkhoyan, T., Ruland, O., De Breuker, R., and Wang, X., "On-Line Black-Box Aerodynamic Performance Optimization for a Morphing Wing With Distributed Sensing and Control," *IEEE Transactions on Control Systems Technology*, Vol. 31, No. 3, 2023, pp. 1063–1077. https://doi.org/10.1109/TCST.2022.3210164.

[8] Hansen, N., and Ostermeier, A., "Completely derandomized self-adaptation in evolution strategies." *Evolutionary computation*, Vol. 9, No. 2, 2001, pp. 159–195. https://doi.org/10.1162/106365601750190398.

[9] Faggiano, F., Vos, R., Baan, M., and Van Dijk, R., "Aerodynamic design of a flying V aircraft," *17th AIAA Aviation Technology, Integration, and Operations Conference, 2017*, , No. June, 2017. https://doi.org/10.2514/6.2017-3589.

[10] Xiong, J., Nguyen, N. T., and Bartels, R. E., "Numerical Simulation of An Aspect Ratio 13.5 Common Research Model with Trailing Edge Mini-Flaps," *AIAA AVIATION 2023 Forum*, 2023, p. 4525. https://doi.org/10.2514/6.2023-4525.

[11] Hanke, C. R., and Nordwall, D. R., "The Simulation of a Large Jet Transport Aircraft. Volume II: Modeling Data," *NASA Contractor Report*, Vol. CR-114494, 1970. https://ntrs.nasa.gov/citations/19730001300.

[12] Vos, R., "Modified from: Flying-V - Flying long distances energy-efficiently," , 2022. https://www.tudelft.nl/en/ae/flying-v [Accessed: May 16, 2024].

[13] Asaro, S., and Vos, R., "Aerodynamic Model for a Flying Wing Aircraft," *Preprint, submitted to AIAA Scitech 2025 Forum*, 2025.

[14] Gomroki, M. M., Topputo, F., Bernelli-Zazzera, F., and Tekinalp, O., "Solving constrained optimal control problems using state-dependent factorization and chebyshev polynomials," *Journal of Guidance, Control, and Dynamics*, Vol. 41, No. 3, 2018, pp. 618–631. https://doi.org/10.2514/1.G002392.

[15] Ruland, O., Mkhoyan, T., De Breuker, R., and Wang, X., "Black-Box Online Aerodynamic Performance Optimization for a Seamless Wing with Distributed Morphing," *Journal of Guidance, Control, and Dynamics*, Vol. 46, No. 3, 2023, pp. 560–570. https://doi.org/10.2514/1.G006573.

[16] Tol, H. J., De Visser, C. C., Van Kampen, E., and Chu, Q. P., "Nonlinear multivariate spline-based control allocation for high-performance aircraft," *Journal of Guidance, Control, and Dynamics*, Vol. 37, No. 6, 2014, pp. 1840–1862. https://doi.org/10.2514/1.G000065.

[17] de Visser, C., "Global Nonlinear Model Identification with Multivariate Splines," Phd thesis, Delft University of Technology, July 2011. Available at https://repository.tudelft.nl/islandora/object/uuid%3A6bc0134a-0715-4829-903d-6479c5735913.

[18] Calise, A. J., and Rysdyk, R. T., "Nonlinear Adaptive Flight Control Using Neural Networks," *IEEE Control Systems*, Vol. 18, No. 6, 1998, pp. 14–25. https://doi.org/10.1109/37.736008.

[19] Calise, A. J., Lee, S., and Sharma, M., "Development of a Reconfigurable Flight Control Law for Tailless Aircraft," *Journal of Guidance, Control, and Dynamics*, Vol. 24, No. 5, 2001, p. 896–902. https://doi.org/10.2514/2.4825.

[20] van den Aarssen, M. S., Visser, T., and de Visser, C. C., "Distributed approach for aerodynamic model identification of the ice aircraft using the alternating direction method of multipliers in combination with simplotope b-splines," *AIAA Scitech 2019 Forum*, 2019. https://doi.org/10.2514/6.2019-1320.

[21] Babuška, R., and Verbruggen, H., "Neuro-fuzzy methods for nonlinear system identification," *Annual Reviews in Control*, Vol. 27 I, No. 1, 2003, pp. 73–85. https://doi.org/10.1016/S1367-5788(03)00009-9.

[22] De Weerdt, E., De Visser, C. C., Chu, Q. P., and Mulder, J. A., "Fuzzy simplex splines," *IFAC Proceedings Volumes (IFAC-PapersOnline)*, Vol. 15, No. PART 1, 2009, pp. 1340–1345. https://doi.org/10.3182/20090706-3-fr-2004.00223.

[23] De Visser, C. C., Mulder, J. A., and Chu, Q. P., "Global nonlinear aerodynamic model identification with multivariate splines," *AIAA Atmospheric Flight Mechanics Conference*, , No. August, 2009. https://doi.org/10.2514/6.2009-5726.

[24] De Visser, C., Mulder, J., and Chu, Q., "A Multidimensional Spline Based Global Nonlinear Aerodynamic Model for the Cessna Citation II," 2010. https://doi.org/10.2514/6.2010-7950.

[25] De Visser, C., Mulder, J., and Chu, Q., "Validating the Multidimensional Spline Based Global Aerodynamic Model for the Cessna Citation II," 2011. https://doi.org/10.2514/6.2011-6356.

[26] Ruiz-García, A., Vos, R., and de Visser, C. C., "Aerodynamic model identification of the flying V from wind tunnel data," *Aiaa Aviation 2020 Forum*, Vol. 1 PartF, 2020, pp. 1–18. https://doi.org/10.2514/6.2020-2739.

[27] Sobol, I., "On the distribution of points in a cube and the approximate evaluation of integrals," *USSR Computational Mathematics and Mathematical Physics*, Vol. 7, No. 4, 1967, pp. 86–112. https://doi.org/10.1016/0041-5553(67)90144-9.

[28] Pardalos, P. M., Rasskazova, V., and Vrahatis, M. N., *Black Box Optimization, Machine Learning, and No-Free Lunch Theorems*, 2021. https://doi.org/10.1007/978-3-030-66515-9.

[29] Rios, L. M., and Sahinidis, N. V., "Derivative-free optimization: A review of algorithms and comparison of software implementations," *Journal of Global Optimization*, Vol. 56, No. 3, 2013, pp. 1247–1293. https://doi.org/10.1007/s10898-012-9951-y.

[30] Powell, M. J. D., "The BOBYQA algorithm for bound constrained optimization without derivatives," 2009. https://api.semanticscholar.org/CorpusID:2488733.

[31] Jones, D. R., Perttunen, C. D., and Stuckman, B. E., "Lipschitzian optimization without the Lipschitz constant," *Journal of Optimization Theory and Applications*, Vol. 79, No. 1, 1993, pp. 157–181. https://doi.org/10.1007/BF00941892.

[32] Vaz, A. I. F., and Vicente, L. N., "A particle swarm pattern search method for bound constrained global optimization," *Journal of Global Optimization*, Vol. 39, No. 2, 2007, pp. 197–219. https://doi.org/10.1007/s10898-007-9133-5.

[33] Xiong, J., Bartels, R. E., and Nguyen, N., "Aerodynamic optimization of mach 0.745 transonic truss-braced wing aircraft with variable-camber continuous trailing-edge flap," *AIAA Scitech 2021 Forum*, , No. January, 2021, pp. 1–22. https://doi.org/10.2514/6.2021-0337.

[34] Eurocontrol, "A359," , 2018. https://contentzone.eurocontrol.int/aircraftperformance/details.aspx?ICAO=A359 [Accessed: September 18, 2024].

# Part III

## Additional Results & Conclusion

# 4

# Additional results

This chapter presents an additional study that did not make it to the scientific paper. First, a study on how effective the optimization framework is at mitigating the pitch brake phenomenon is presented in Section 4.1. In addition, a small discussion on the application of this optimization framework to real aircraft is given in Section 4.2.

## 4.1. Morphing wings for pitch brake mitigation

When looking at the $C_M - \alpha$ curve, one can see a high degree of nonlinearity at a higher angle of attack and a switch point after which $C_{M_\alpha}$ becomes positive. For stability reasons, $C_{M_\alpha}$ is desired to be negative because this will counteract any disturbances to the stable (trim) condition. However, that is not the case for the Flying-V as with higher angles of attack the $C_{M_\alpha}$ becomes positive. This behavior is called pitch brake. The main optimization variable (in this study) that is related to pitch brake is the angle of attack. For this reason, a study is done to see whether the optimization framework is capable of delaying the conditions where pitch brake arises by lowering the angle of attack. Having a morphing wing allows the aircraft to get more lift from the inner control surfaces, while the outer part of the wing can maintain trim.

A second cost function has been made that adds a penalty for higher angles of attack, thus favouring feasible solution with the lowest angle of attack possible. This cost function can be described as follows:

$$J_2(\alpha, \boldsymbol{\delta}) = C_D + k_1(C_{L,\text{target}} - C_L)^2 + k_2(C_M)^2 + k_3\alpha \tag{4.1}$$

where $\alpha$ is the angle of attack, $\boldsymbol{\delta}$ the flap deflections, and $k_1$ and $k_2$ the deviations from target lift and moment coefficients respectively. Figure 4.7 shows the results of this cost function compared to the normal cost function (from the scientific paper). Since the original cost function already tends to converge to solutions with a low angle of attack, the added benefit of the pitch brake cost function is rather low. When optimizing for drag reduction, the main parameter that the system wants to lower is the angle of attack. Any extra penalties will not work, or prefer the smaller angle of attack over being in trim. So unfortunately, this is not a feasible method to delay the angle at which pitch brake happens.

## 4.2. Application in real aircraft

In the current study, the system has been tested and validated within a simulated environment. However, for real-world applications, different sensing equipment is required because the force balance used in the simulation setup cannot be applied to a free-flying aircraft. In real flight conditions, aerodynamic forces such as lift and drag must be estimated using onboard sensors. These forces can be inferred from measurable parameters like the aircraft's weight, pitch angle, angle of attack, fuel consumption, and thrust-specific fuel consumption (TSFC), which vary with flight speed and altitude. Potential alternatives to a force-balance system in real-world scenarios include the use of strain gauges, fiber optics [13], or model-based load estimation, where parameters such as angle of attack, flight speed, and fuel flow are used to calculate forces. With appropriate modifications to the sensing equipment, the methodology could be extended to actual commercial aircraft.

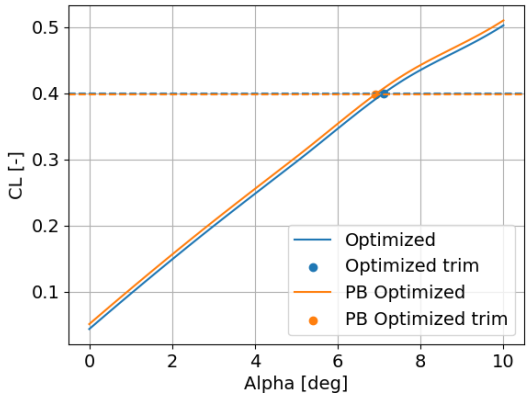


**Figure 4.1:** CL vs Angle of Attack

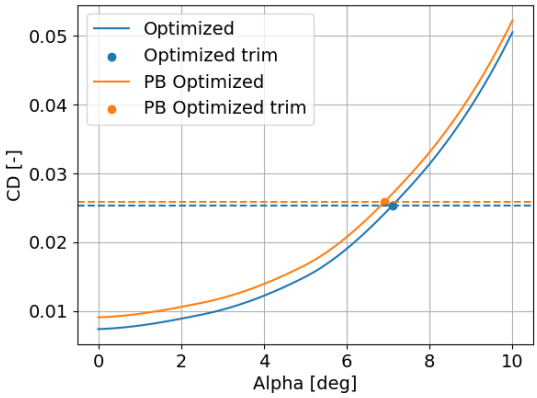


**Figure 4.2:** CD vs Angle of Attack

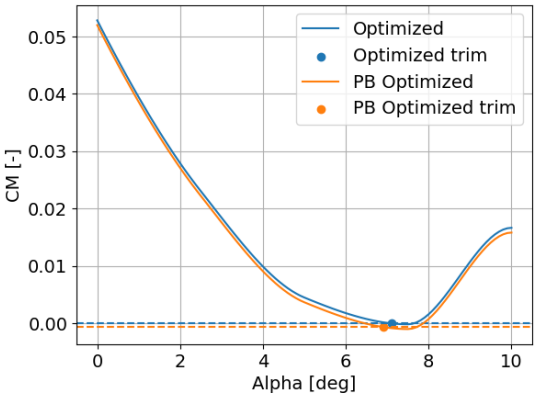


**Figure 4.3:** CM vs Angle of Attack

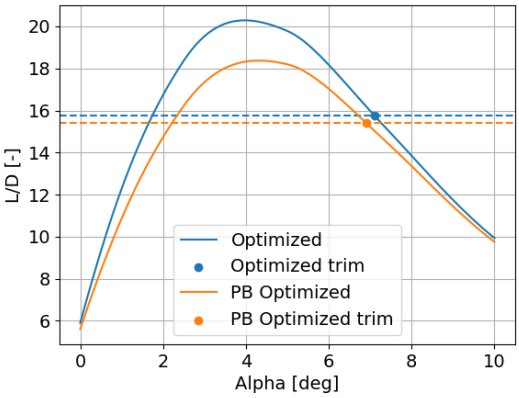


**Figure 4.4:** L/D vs Angle of Attack

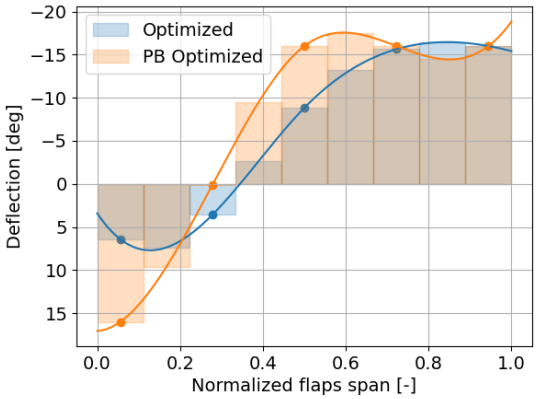


**Figure 4.5:** Deflections

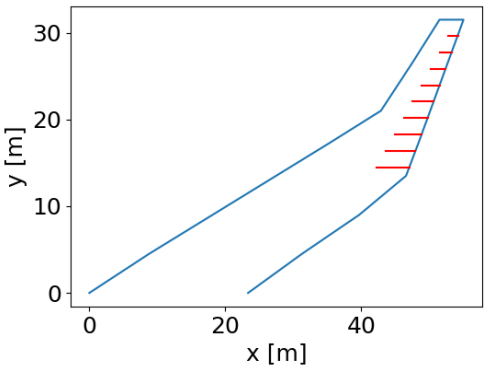


**Figure 4.6:** Morphing actuator locations

**Figure 4.7:** Optimized results of pitch brake optimization (PB Optimized) compared to normal optimization for $C_{L_{\text{target}}} = 0.26$, Mach $= 0.7$

# 5

# Conclusions & Recommendations

This chapter presents the key conclusions drawn from the research and outlines recommendations for future work. The conclusions are drawn by revisiting the research questions introduced in Chapter 3. The chapter also highlights the limitations encountered during the study, offering recommendations for overcoming these challenges in future research.

## 5.1. Conclusions

The research questions posed in Chapter 3 are repeated below and a conclusion can be made on how it was addressed and what the results were of every research question. In the end, a conclusion will be made on the total thesis.

**Research Question 1**

How to design an optimization architecture that is best suited for online shape optimization?

A feedback optimization architecture was created that consisted of the following items:

- **Optimizer:** For the optimizer a trade-off was done that concluded that the thrust-region method BOBYQA was best suited for this optimization task. The need for global optimization was made clear through a sensitivity analysis of different runs and the non-convex nature of the optimization. In addition, BOBYQA outperformed the other global optimization methods due to its quick convergence and high performance.
- **On-board model:** For the on-board model three popular methods were presented. Splines were chosen as model identification method due to the ability of modelling local complex behavior while keeping the computational loads low. In addition, it provides more transparent behavior than neural networks. The spline-based model identification resulted in a successful choice as it could adequately model the Flying-V.
- **Cost function:** For the cost function a simple option was presented that aims to keep the drag as low as possible, while maintaining $C_L = C_{L_{\text{target}}}$ and $C_M = 0$. This also proved to be successful in seeking the most optimal solution.
- **Aircraft Aerodynamics:** For the aircraft aerodynamics a combination of high fidelity RANS simulations and low fidelity VLM simulations were used, in addition to wind tunnel data to tune the coefficients. While VLM simulations have some limitations associated with them, the overall method still holds up due to the main part being reliant on high-fidelity solvers.
- **Spline conversion:** A spline conversion was added to decrease the number of optimization variables from the number of actuators to just 5. This proved to be a successful method as a spline function can model most shapes while keeping smoothness.

**Research Question 2**

How can the optimizer best account for actuator failures?

A method was suggested to have the optimization framework automatically detect an actuator failure, adapt the on-board model, and optimize the remaining flaps. The system's ability to handle these failures is broken down into three key aspects:

- **Detecting Actuator Failures**: The optimizer incorporates a mechanism that continuously monitors the discrepancy between the onboard model and real-time aerodynamic performance. When a failure occurs, it detects this by comparing expected outputs (trimmed flight condition) with actual flight data. If a mismatch arises, the system concludes that an actuator failure might have occurred.
- **Identifying the Failed Actuator**: Once a failure is detected, the optimizer runs a sequence of model excitations to adapt the on-board model. When a particular actuator shows no influence on the aerodynamic performance (e.g. the lift contribution becomes negligible), it is marked as the faulty actuator.
- **Optimizing the Remaining Actuators**: After identifying the failed actuator, the system adapts by modifying the control variables to exclude the failed actuator from the optimization loop. The remaining actuators are then re-optimized to maintain trim and optimal aerodynamic performance.

**Research Question 3**

Compared to non-morphing wings, what are the efficiency gains for any point in the flight profile?

The efficiency gains over the whole flight profile were also addressed in the study and resulted in a clear idea of where the continuous trailing edge flaps have most optimization capabilities. From the study it can be concluded that the optimization framework reaches higher L/D ratio increases at higher target lift coefficients. The reason for this is that at higher target lift coefficients, the actuators can utilize more of its range to optimize both for the drag while keeping the aircraft in trim. As opposed to low target lift coefficients where the actuators had a more horizontal shape which could be easily achieved by a single-actuator system as well. The flight phases were estimated using public rate of climb data from the Airbus A359. A better view of the efficiency gains can be achieved when using a flight profile that is more relevant to the Flying-V and also uses a better weight model estimation to get the target lift coefficients for every flight phase.

In conclusion, this thesis has proposed a global online data-driven aerodynamic performance optimization framework, which can efficiently and smoothly model nonlinearities, adapt to changes on-board in real-time, and automatically detect and adapt to actuator faults. This thesis has demonstrated several significant advancements in aerodynamic optimization for morphing wings as applied on the TU Delft Flying-V. The key findings underscore the system's ability to achieve a drag reduction of 1.9% to 4.9% during cruise. At higher target lift coefficients (caused by heavier weight and lower speed), the drag reduction can reach up to 12.6%. These results confirm that the combination of the model-based optimization algorithm BOBYQA and a multivariate spline-based on-board model is effective in solving the optimization problem. Additionally, the investigation into fault redundancy showed that the system retains the ability to optimize performance even in the presence of actuator failures, providing robust fault tolerance. The trade-off analysis between actuator configurations revealed that a setup with 6 to 9 actuators is the most advantageous, striking a balance between drag reduction and the added weight of additional actuators.

## 5.2. Recommendations

The research also has its limitations. First, the system did not improve on existing model excitation techniques. Current methods require either low frequency excitation that allow enough time to keep the aircraft in trim, or use high frequency excitations that add unwanted disturbances to any passengers. Ideally, these model excitations are only necessary during test flights, but with extra actuator failure detection methods the aircraft requires to update the on-board model at any time. Additionally, manual input is still needed to define the flight conditions. Future studies could look into the merger of contextual learning and optimization, such that the altitude and Mach number are included in the optimization strategy. Another limitation is that the optimization process is restricted to trailing edge morphing only. Expanding the control surfaces used in the optimization could provide greater flexibility and potentially further reduce drag. Additionally, future research could involve higher fidelity solvers to further refine the optimization and improve its accuracy.

While the optimization framework is fit to be applied to real-world commercial aircraft on a real aircraft, there needs to be further research on how to implement aerodynamic forces and coefficients extractions during flight. This thesis has the benefit that everything is done in simulation, thus the coefficients are easily calculated. Potential methods for real-world implementation could involve the use of strain gauges, fiber optics, or a combination of these technologies [13]. Additionally, model-based load estimation using other measurable parameters, such as angle of attack, flight speed, altitude, and fuel flow, is also a viable approach.

Overall, these limitations do not detract from the overall success of the study but rather point to areas for improvement in future work.

# References


[1] Tigran Mkhoyan et al. “Design and development of a seamless smart morphing wing using distributed trailing edge camber morphing for active control”. In: *AIAA Scitech 2021 Forum* (2021), pp. 1–16. DOI: 10.2514/6.2021-0477.

[2] Glenn B. Gilyard et al. “Flight test of an adaptive configuration optimization system for transport aircraft”. In: *37th Aerospace Sciences Meeting and Exhibit* January (1999). DOI: 10.2514/6.1999-831.

[3] Marianne Jacobsen. “Real time drag minimization using redundant control surfaces”. In: *Aerospace Science and Technology* 10.7 (2006), pp. 574–580. DOI: 10.1016/j.ast.2006.05.002.

[4] Nhan Nguyen. “NASA Innovation Fund 2010 Project Elastically Shaped Future Air Vehicle Concept”. In: *NASA Technical report* (2010). https://ntrs.nasa.gov/citations/20110023698.

[5] Yvonne Ferrier et al. “Real-time adaptive least-squares drag minimization for performance adaptive aeroelastic wing”. In: *34th AIAA Applied Aerodynamics Conference* (2016), pp. 1–33. DOI: 10.2514/6.2016-3567.

[6] Nhan Nguyen et al. “Real-time adaptive drag minimization wind tunnel investigation of a flexible wing with variable camber continuous trailing edge flap system”. In: *AIAA Aviation 2019 Forum* June (2019), pp. 1–47. DOI: 10.2514/6.2019-3156.

[7] Nhan Nguyen et al. “Real-time drag optimization of aspect ratio 13.5 common research model with distributed flap system”. In: *AIAA Scitech 2021 Forum* January (2021), pp. 1–17. DOI: 10.2514/6.2021-0069.

[8] Juntao Xiong et al. “Aerodynamic optimization of mach 0.745 transonic truss-braced wing aircraft with variable-camber continuous trailing-edge flap”. In: *AIAA Scitech 2021 Forum* January (2021), pp. 1–22. DOI: 10.2514/6.2021-0337.

[9] Nhan Nguyen et al. *Real-time drag optimization control framework*. US-11242134-B1, Feb. 2022. URL: https://ppubs.uspto.gov/dirsearch-public/print/downloadPdf/11242134.

[10] Oscar Ruland et al. “Black-Box Online Aerodynamic Performance Optimization for a Seamless Wing with Distributed Morphing”. In: *Journal of Guidance, Control, and Dynamics* 46.3 (2023), pp. 560–570. DOI: 10.2514/1.G006573.

[11] Tigran Mkhoyan et al. “On-Line Black-Box Aerodynamic Performance Optimization for a Morphing Wing With Distributed Sensing and Control”. In: *IEEE Transactions on Control Systems Technology* 31.3 (2023), pp. 1063–1077. DOI: 10.1109/TCST.2022.3210164.

[12] N. Hansen et al. “Completely derandomized self-adaptation in evolution strategies.” In: *Evolutionary computation* 9.2 (2001), pp. 159–195. DOI: 10.1162/106365601750190398.

[13] J.-H. Kim et al. “Aircraft health and usage monitoring system for in-flight strain measurement of a wing structure”. In: *Smart Materials and Structures* 24.10 (2015), p. 105003. DOI: 10.1088/0964-1726/24/10/105003.

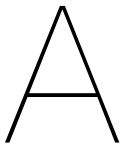

# Project planning

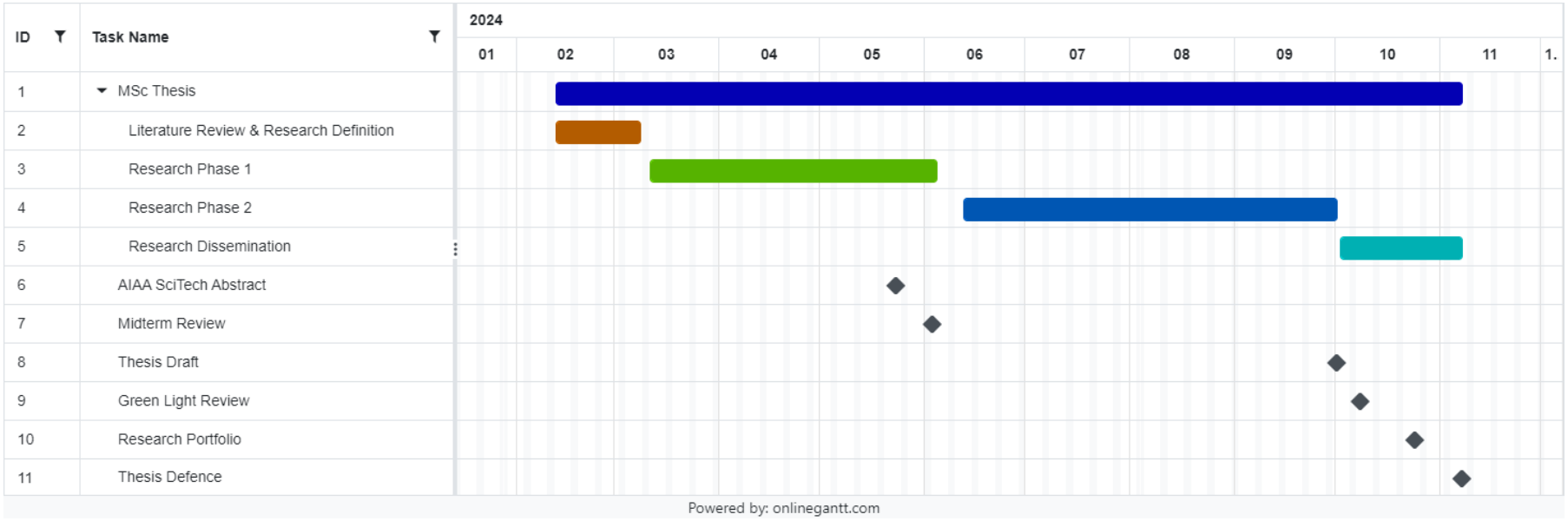


**Figure A.1:** Project outline Gantt chart